

3 16
3 25.63

DP - 817

Physics

AEC Research and Development Report

RESONANCE INTEGRALS AND SELF-SHIELDING FACTORS FOR DETECTOR FOILS

by

N. P. Baumann
Experimental Physics Division

MASTER

January 1963

E. I. du Pont de Nemours & Co.
Savannah River Laboratory
Aiken, South Carolina

This document is
PUBLICLY RELEASABLE
David Bellis /
Authorizing Official b1
Date: 7-7-04

DISCLAIMER

This report was prepared as an account of work sponsored by an agency of the United States Government. Neither the United States Government nor any agency Thereof, nor any of their employees, makes any warranty, express or implied, or assumes any legal liability or responsibility for the accuracy, completeness, or usefulness of any information, apparatus, product, or process disclosed, or represents that its use would not infringe privately owned rights. Reference herein to any specific commercial product, process, or service by trade name, trademark, manufacturer, or otherwise does not necessarily constitute or imply its endorsement, recommendation, or favoring by the United States Government or any agency thereof. The views and opinions of authors expressed herein do not necessarily state or reflect those of the United States Government or any agency thereof.

DISCLAIMER

Portions of this document may be illegible in electronic image products. Images are produced from the best available original document.

This report was prepared as an account of Government sponsored work. Neither the United States, nor the Commission, nor any person acting on behalf of the Commission:

- A. Makes any warranty or representation, expressed or implied, with respect to the accuracy, completeness, or usefulness of the information contained in this report, or that the use of any information, apparatus, method, or process disclosed in this report may not infringe privately owned rights; or
- B. Assumes any liabilities with respect to the use of, or for damages resulting from the use of any information, apparatus, method, or process disclosed in this report.

As used in the above, "person acting on behalf of the Commission" includes any employee or contractor of the Commission, or employee of such contractor, to the extent that such employee or contractor of the Commission, or employee of such contractor prepares, disseminates, or provides access to, any information pursuant to his employment or contract with the Commission, or his employment with such contractor.

Printed in USA. Price \$1.25
Available from the Office of Technical Services
U. S. Department of Commerce
Washington 25, D. C.

DP-817

PHYSICS
(TID-4500, 18th Ed.)

RESONANCE INTEGRALS AND SELF-SHIELDING
FACTORS FOR DETECTOR FOILS

by

Norman P. Baumann

January 1963

E. I. du Pont de Nemours & Co.
Explosives Department - Atomic Energy Division
Technical Division - Savannah River Laboratory
Aiken, South Carolina

Contract AT(07-2)-1 with the
United States Atomic Energy Commission

Approved by
J. L. Crandall, Research Manager
Experimental Physics Division

ABSTRACT

Effective activation resonance integrals for thin and thick foils in an isotropic neutron flux were measured by a cadmium ratio method. Gold was used as a standard. Values obtained for dilute resonance integrals in barns, not including 1/v capture, were: Au¹⁹⁷, 1390 ±40 (Reference); U²³⁸ capture, 280 ±10; Cu⁶³, 3.17 ±0.18; Cu⁶⁵, 1.39 ±0.22; Mo⁹⁸, 9.9 ±1.1; Mo¹⁰⁰, 4.06 ±0.23; W¹⁸⁶, 476 ±50; and Na²³, 0.075 ±0.010. Dilute resonance integrals including 1/v capture above 0.60 ev were: U²³⁵ fission, 263 ±9 and In¹¹⁵, 3200 ±100. These resonance integrals and the measured resonance flux self-shielding factors were generally in good agreement with calculations. However, the two isotopes of molybdenum appeared to have major contributions to their resonance integrals from nontabulated resonances.

CONTENTS

	<u>Page</u>
List of Tables	4
List of Figures	5
Introduction	6
Summary	6
Discussion	8
Theoretical	8
Definition of Resonance Integral	8
Method of Measurement	9
Technique	11
Method (Experimental)	11
Gold Calibration	13
Effective Resonance Integrals	16
Cu^{63} and Cu^{65}	16
Mo^{98} and Mo^{100}	19
Na^{23}	23
U^{235} Fission	25
U^{238} Capture	27
In^{115}	31
W^{186}	34
Neutron Spectrum in the SP	36
Appendix A - Calculation of Flux Depression Factors	37
Appendix B - Effective Cadmium Cutoff Energies	43
Appendix C - Method for Determining Cadmium Ratios of Short-Lived Isotopes	44
Appendix D - Determination of the Effective Resonance Energy for Mo^{98} and Mo^{100}	46
Bibliography	49

LIST OF TABLES

<u>Table</u>		<u>Page</u>
I	Dilute Resonance Activation Integrals for Various Detector Materials	7
II.	Computed Resonance and Thermal Depression Factors for Gold Foil Activations in an Isotropic Flux in a Cavity	15
III	Measured Cadmium Ratios and Resonance Integrals for Cu ⁶³ and Cu ⁶⁵	18
IV	Measured Cadmium Ratios and Resonance Integrals for Mo ⁹⁸ and Mo ¹⁰⁰	20
V	Resonance Integrals for Mo ⁹⁸ and Mo ¹⁰⁰	22
VI	Measured Cadmium Ratios and Resonance Integrals for Na ²³	25
VII	Measured Cadmium Ratios and Resonance Integrals for U ²³⁸ Capture	29
VIII	Comparison of the Thermal and Resonance Activation Cross Sections for the 13-Second and 54-Minute Activities of In ¹¹⁶	32
IX	Computed Resonance and Thermal Depression Factors for In ¹¹⁵ Activations in an Isotropic Flux in a Cavity	33

LIST OF FIGURES

<u>Figure</u>	<u>Page</u>
1 Foil Irradiation Apparatus	12
2 Thickness Corrections for Cadmium Ratios of Au ¹⁹⁷ Foils (Isotropic Flux in Cavity)	15
3 Effective Resonance Integral for Cu ⁶³ and Cu ⁶⁵ as a Function of Foil Thickness (Isotropic Flux in Cavity)	18
4 Effective Resonance Integral for Mo ⁹⁰ and Mo ¹⁰⁰ as a Function of Foil Thickness (Isotropic Flux in Cavity)	21
5 Effective Resonance Capture Integral for U ²³⁸ as a Function of Foil Thickness (Isotropic Flux in Cavity)	31
6 Thickness Corrections for Cadmium Ratios of In ¹¹⁵ and W ¹⁸⁶ Foils (Isotropic Flux in Cavity)	34
7 Flux Depression Factors for Thin Foils with No Doppler Broadening	39
8 Resonance Flux Dépression Factors for Thick Foils with No Doppler Broadening	40
9 Resonance Flux Depression Factors for Thin Foils with Doppler Broadening Included	42
10 Resonance Flux Depression Factors for Thick Foils with Doppler Broadening Included	42
11 Effective Cadmium Cutoff Energies for Thin 1/v Detector Foils	43
12 Shielding of Resonance Detector Foils by Boron Covers	48

RESONANCE INTEGRALS AND SELF-SHIELDING FACTORS FOR DETECTOR FOILS

INTRODUCTION

Resonance detector foils are an essential tool for reactor physics measurements. However, their usefulness depends on the precision with which their resonance parameters are known. Such parameters include the resonance energy, resonance width, resonance integral, and self-shielding factors. The resonance energies and reaction widths are generally available⁽¹⁾ from neutron cross section measurements for the energy regions in which resonances for various isotopes can be resolved. Reasonably complete summaries of resonance integrals have also been published^(2,3), but resonance integral measurements are subject to sizable errors arising from self-shielding effects, non-1/E spectra, and other sources.

The present experiments were undertaken to obtain precise measurements of resonance integrals for some of the more commonly used resonance detectors. The experiments were designed to give the dilute, or unshielded, resonance integrals as well as to give the variation of the effective resonance integral with foil thickness over commonly used thickness ranges.

SUMMARY

Measurements and calculations of resonance integrals and flux depression factors have been made for foil activations in U^{235} , U^{238} , W^{186} , In^{115} , Na^{23} , Cu^{63} , Cu^{65} , Mo^{98} , and Mo^{100} . Measurements were made by the "cadmium ratio" method, with Au^{197} as the reference material. The infinite dilution activation integrals are given in Table I.

The resonance flux depression factors were calculated as a function of foil thickness for those materials whose resonance parameters were available. The calculations included the effect of Doppler broadening but neglected the effect of resonance scattering. The agreement with experiment was extremely good for U^{238} , In^{115} , Au^{197} , Mo^{98} , and Mo^{100} . A marked disparity was observed for W^{186} , which is qualitatively explained by the very large scattering component of the tungsten resonance. Computations of self-shielding effects for the copper isotopes were not made because sufficient data for the resonances were not available. The resonance self-shielding for Na^{23} and U^{235} was negligible for the foil thicknesses used.

Special methods were devised to treat the special problems imposed by the various foil materials. For W^{186} , a resonance in Cd^{113} overlaps the 18.8-ev resonance. Measurements of the resultant shielding were made by comparing cadmium ratios of the tungsten activity with similar boron ratios. The boron measurements gave resonance integrals for W^{186} about 24% greater than those derived from the cadmium measurements. For In^{115} , neutron capture leads to two modes of decay; one with a 54-minute half-life, the other with a 13-second half-life. The branching ratio of the two modes for thermal neutron capture has been published⁽¹⁾, but a report of such measurements for epicadmium captures could not be found. This determination was made in the present experiment by comparison of cadmium ratios for the two activities. A special double counter method was used to obtain precise activity ratios for the 13-second activity. The measured resonance integral of Mo^{98} greatly exceeded that calculated from the parameters of the single tabulated resonance. Measurements were undertaken with successive thickness of boron shielding to try to locate the difficulty. These experiments showed that a major portion of the Mo^{98} resonance integral originated at an energy in the vicinity of 100 ev, well below the tabulated resonance of 480 ev. They also indicated that Mo^{100} has significant resonance integral contributions at energies much higher than the tabulated resonance at 367 ev. Until the unknown resonances are identified, neither of these molybdenum isotopes appears useful as a resonance detector.

TABLE I
Dilute Resonance Activation
Integrals for Various Detector Materials

Isotope	$g \sigma_{th}$, barns ^(a)	RI^{Res} , barns ^(b)
Au^{197} (Reference)	99.4	1490 ± 40
Na^{23}	0.52	0.075 ± 0.010
Cu^{63}	4.5	3.17 ± 0.18
Cu^{65}	2.0	1.39 ± 0.22
Mo^{98}	0.18	9.9 ± 1.1
Mo^{100}	0.199	4.06 ± 0.23
W^{186}	35	476 ± 50
U^{238} (Capture)	2.73	280 ± 10
U^{235} (Fission)	561	263 ± 9
In^{115} (54M)	156	2550 ± 80
In^{115} (13S)	38.7	650 ± 30

(a) Values of Resonance Integrals are directly proportional to value of $g \sigma_{th}$ assumed. For revisions of thermal cross sections, revised resonance integrals should be used.

(b) Resonance Integrals do not include epicadmium $1/v$ capture except for U^{235} ($E_{cd} = 0.600$ ev) and In^{115} ($E_{cd} = 0.622$ ev).

DISCUSSION

THEORETICAL

DEFINITION OF RESONANCE INTEGRAL

The resonance absorption integral is an index of the epithermal neutron absorption by a material in a reactor flux. Since most thermal reactors have an epithermal flux that varies approximately as $1/E$ with the neutron energy, E , resonance integrals are usually defined with respect to such a $1/E$ flux distribution.

If the microscopic absorption cross section of the material is $\sigma_a(E)$, and if there are no self-shielding effects, the total epithermal resonance integral is given by

$$(RI)^{\text{Tot}} = \int_{E_0}^{\infty} \sigma_a(E) \frac{dE}{E} \quad (1)$$

where the lower energy limit E_0 is normally taken to be five times the energy kT which characterizes the Maxwellian thermal flux distribution⁽⁴⁾. The value of kT depends on the temperature; for a temperature of 20°C, kT is 0.0253 ev. The temperature dependence of the resonance integral may be eliminated by any one of several practical devices. One such device is to specify a lower energy limit greater than five times the highest value of kT encountered. A value of $E_0 = 0.5$ ev is frequently used. Another device is to specify a lower energy limit determined by the effective cadmium cutoff energy. While this latter method removes the temperature dependence, it introduces a dependence on cadmium thickness and the degree of flux anisotropy. In addition, this method introduces a dependence on the manner in which the absorption cross section varies with energy in the vicinity of the cadmium cutoff energy (which is at approximately 0.5 ev). For absorbers that have resonances above 3 to 4 ev, the most convenient device is to define RI^{Res} as the total resonance integral minus the $1/v$ component. This quantity is then independent of temperature and of E_0 over a wide range. It may be expressed as

$$(RI)^{\text{Res}} = (RI)^{\text{Tot}} - (RI)^{1/v} \equiv \int_{E_0}^{\infty} \sigma_a(E) \frac{dE}{E} - \int_{E_0}^{\infty} \sigma_{\text{th}} \sqrt{\frac{E_{\text{th}}}{E}} \frac{dE}{E} \quad (2)$$

where σ_{th} is the absorption cross section at the thermal energy, E_{th} .

PAGES 9 to 10

WERE INTENTIONALLY
LEFT BLANK

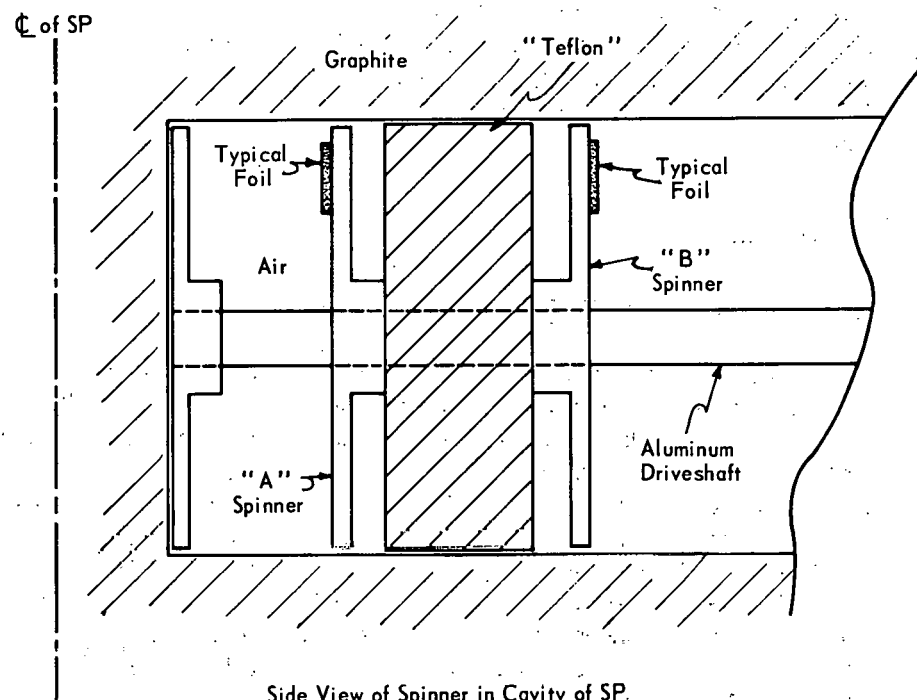
for this effect are 0.985 for gold and 0.937 for indium at a cadmium thickness of 0.030 inch. Corrections for W^{186} are discussed in a later section. Shielding by cadmium is assumed to be negligible for the other detector foils of the present experiment.

TECHNIQUE

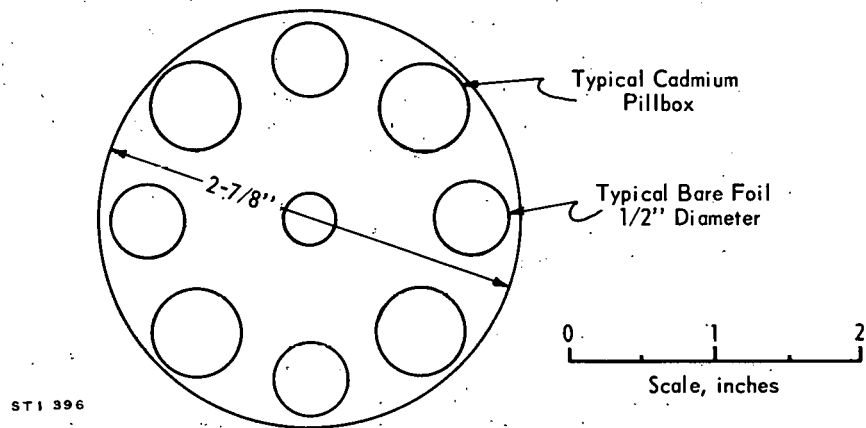
METHOD (EXPERIMENTAL)

Foil activations were made in the Standard Pile (SP) of the Savannah River Laboratory (SRL). The SP^(9,10) is a water-cooled, graphite-moderated reactor, fueled with fully enriched uranium. The construction is similar to that of the Thermal Test Reactor (TTR)⁽¹¹⁾. The irradiations were conducted in the central thimble, a 3.00-inch-diameter tube along the axis of the reactor. Solid graphite cylinders 3 inches in diameter were loaded in one end of the central thimble up to 3/4 inch past the reactor midplane. The remainder of the thimble contained the foil holders as indicated in Figure 1. Foils were affixed to the aluminum spinner discs with a single thickness of cellophane tape. Four bare and four cadmium-covered foils were placed on each disc. The aluminum rod and a series of "Teflon" blocks served as a mandrel so that the spinner discs could be rotated during the irradiations, thus eliminating the effect of possible flux gradients across the cavity. The endmost spinner disc served to position the holder. During the irradiations just enough pressure was applied to keep this disc in contact with the graphite end face. This allowed accurate repositioning after removal of the holding apparatus.

The structural materials of the irradiation apparatus were selected for their nuclear as well as their mechanical properties. Both aluminum and "Teflon" have low slowing down powers, small thermal neutron absorption cross sections, small scattering cross sections, and negligible resonance effects. The full set of eight cadmium covers was used in each irradiation whether or not the full eight sets of foils were used. This served to standardize the thermal neutron flux depression in the vicinity of the cavity since the variation in total neutron absorption in the cavity due to the different foils was negligible compared to the constant absorption of the cadmium and the structural materials. The cadmium covers were in the form of cylindrical pillboxes and were 0.030 inch thick on each face as well as at the edge.



Side View of Spinner in Cavity of SP.



End View of Aluminum Foil Holding Disc

FIG. 1 FOIL IRRADIATION APPARATUS

GOLD CALIBRATION

The method of measuring resonance integrals by cadmium ratios requires the use of a reference material whose thermal cross section and resonance integral are precisely known. In principle, a material whose activation cross section has a $1/v$ energy dependence would be an ideal standard except that no such material exists, and if it did, its use would require a knowledge of the precise effective cadmium cutoff energy. What is actually done is to use an activating reference material that has itself been calibrated to a boron counter as the $1/v$ detector. Recent measurements by Jirlow and Johansson⁽⁷⁾ of the resonance integral of gold now make gold a suitable reference material. In those measurements a beam flux permitted the comparison to be made between the gold activations and boron counters of conventional size and shape. In addition the effective cadmium cutoff energy was determined by means of a neutron chopper. They have thus given a careful calibration of gold in terms of a $1/v$ absorber. The value obtained for the total epicadmium resonance activation integral for infinitely thin gold foils was 1535 ± 40 barns, based on a thermal cross section of 98.8 barns and a cutoff energy of 0.49 ev.

In the present experiment, half-inch-diameter gold foils of approximately 10 mg/cm^2 were used as the basic reference foils. Foil thicknesses were determined by weighing the individual foils. Since foil thicknesses varied by as much as 10% from foil to foil and since this difference in foil thickness is sufficient to cause appreciable difference in the amount of resonance self-shielding, it was necessary to make a self-shielding correction as well as the normal weight correction to the individual measured cadmium ratios. Although experimental data have been obtained⁽⁸⁾ on which to base such corrections, it was felt that corrections based on calculations from basic resonance parameters would be more accurate. The calculations follow the procedure given in Appendix A and include depressions for the nine strongest resonances, the epicadmium $1/v$ component, and the thermal flux. The effect of Doppler broadening is also included. The results of the calculation are presented in Table II.

The resonance flux is based on a cadmium cutoff energy of 0.622 ev. The expression "flux depression factor" is a shorthand notation to describe the activity per unit weight of the foils relative to the activity per unit weight of an infinitely thin foil.

The data of Table II are shown graphically in Figure 2 where they are compared to the earlier experiments⁽⁹⁾ at the Savannah River Laboratory and to some new measurements. In this figure the experimentally measured quantities, the ratios of $[CR - 1]^0$ for an infinitely thin foil pair to $[CR - 1]^x$, for a foil pair of finite thickness, are compared to the theoretical equivalents, the activation ratios of the last column of Table II. The earlier experimental data have been renormalized to allow for the fact that the calculated extrapolation to zero foil thickness is different from the extrapolation used in the earlier experiment. This renormalization reduces the experimental ratios to 0.980 times the earlier values.

The agreement of the calculated values with the experimental values is very good except in the thickness range from 10 to 30 mg/cm². In order to determine whether the experiment or the calculation is in error in this range, a remeasurement with both thin and thick gold foils (0.22 and 10 mg/cm²) was made under the present experimental conditions. Cadmium ratios were taken first with the paired foils alternately bare and cadmium covered and then with the positions reversed. The geometric mean cadmium ratio of the normal and reversed positions was used after making corrections for the small difference of resonance self-shielding among the thick foils. As seen from Figure 2, the present experiment agrees with the calculated curve. The three data points shown actually represent the average of a total of 18 cadmium ratio measurements. The validity of the calculations may also be demonstrated by comparing the zero thickness cadmium ratios as calculated from the 10 mg/cm² foils to those calculated from the very thin foils. The thicker foils give zero thickness cadmium ratios of 2.005 ± 0.008 for "A" position and 2.086 ± 0.008 for "B" position compared to 2.010 ± 0.010 and 2.093 ± 0.010 for the corresponding cadmium ratios from the very thin foils. The validity of the computed depression factors of Table II is further verified by comparison with recent measurements by Brown⁽¹²⁾, et al. Our computations agree closely with all the experimental points but deviate markedly from the interpolation curve drawn by these authors through their somewhat more limited number of data points.

The thermal cross section, σ_{th} , of gold at 0.0253 ev is taken to be 98.8 barns^(4,7), the value of g in Equation 7 is 1.006 at an estimated neutron temperature of 30°C, and the value of the resonance component of the resonance integral is 1490 ± 40 barns⁽⁷⁾ to which must be added a 1/v component of 40 barns for a cadmium cutoff energy of 0.622 ev. The value of the resonance shielding factor is 0.985 for gold covered by 0.030-inch-thick cadmium⁽⁸⁾. It is important to note that

TABLE II
 Computed Resonance and Thermal Depression Factors
 for Gold Foil Activations in an Isotropic Flux in a Cavity

Foil Thickness, mg/cm ²	Resonance Depression Factor, F^{Res}	Thermal Depression Factor, F^{th}	$F^{\text{Res}}/F^{\text{th}}$
0.05	0.994	1.000	0.994
0.1	0.987	1.000	0.987
0.2	0.975	1.000	0.975
0.5	0.950	1.000	0.950
0.75	0.931	0.999	0.932
1.0	0.919	0.999	0.920
2.0	0.867	0.998	0.869
3.0	0.828	0.997	0.830
5.0	0.763	0.995	0.767
7.5	0.698	0.994	0.702
10	0.645	0.992	0.650
20	0.521	0.985	0.529
40	0.410	0.969	0.423
60	0.347	0.959	0.362
120	0.264	0.930	0.283
240	0.202	0.882	0.229

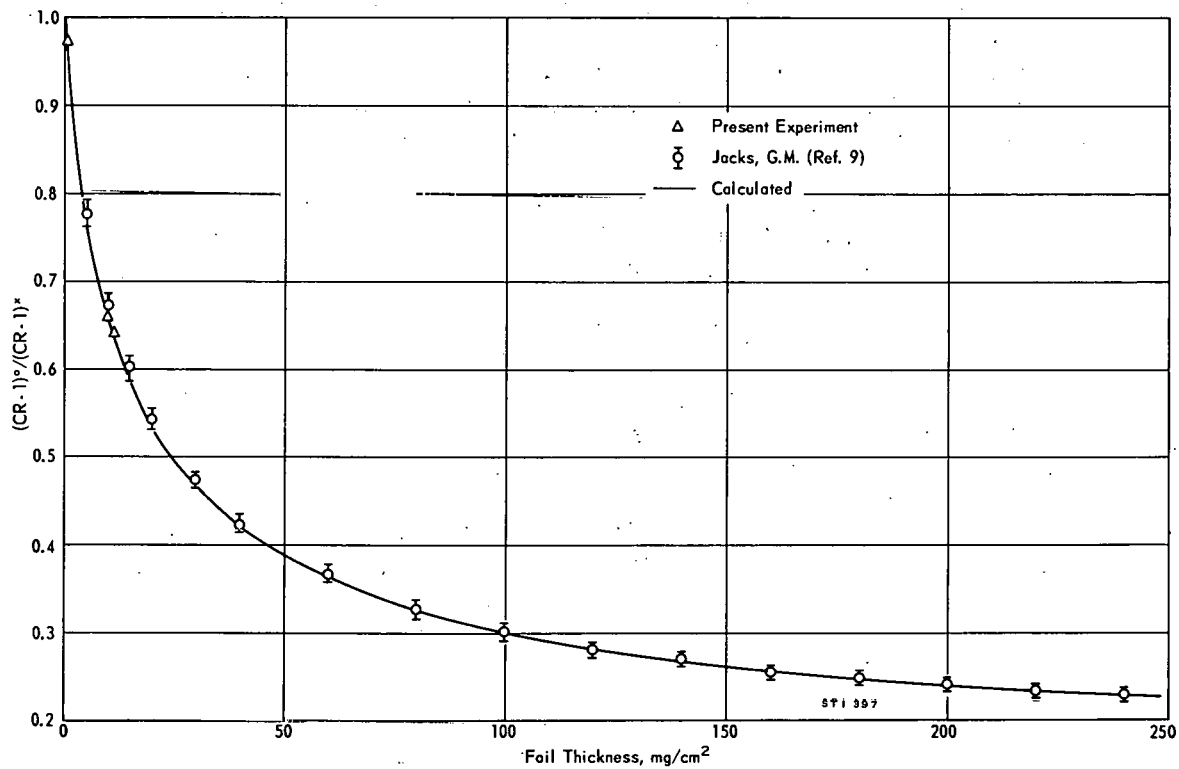


FIG. 2 THICKNESS CORRECTIONS FOR CADMIUM RATIOS OF Au^{197} FOILS
 (Isotropic Flux in Cavity)

this same correction is implicitly made in the reference experiment⁽⁷⁾. From these cross sections and the cadmium ratios derived from the 10 mg/cm² foils one obtains the following calibration relations for the present experiment.

$$\left(\frac{RI_{Tot}}{\sigma_{th}} \right) = 15.00 [CR - 1]^{-1} \quad "A" \text{ Position} \quad (8)$$
$$\left(\frac{RI_{Tot}}{\sigma_{th}} \right) = 16.21 [CR - 1]^{-1} \quad "B" \text{ Position}$$

EFFECTIVE RESONANCE INTEGRALS

Cu⁶³ AND Cu⁶⁵

Copper is frequently used as a neutron poison for reactor experiments. Its utility in this service depends on a precise knowledge of its thermal cross section as well as its resonance integral. Although the thermal cross section of 3.77 \pm 0.04 barns⁽¹³⁾ is known sufficiently accurately, the value of the resonance integral and its dependence on foil thickness have not been measured precisely. An added complication is that two isotopes, Cu⁶³ and Cu⁶⁵, contribute to the resonance integral, but in many reactor experiments only the 12.8-hour activity from neutron capture by Cu⁶³ can be counted conveniently. The results of the present experiment provide the basis for computing the total copper absorption from measurements of the 12.8-hour activity alone.

Foils were made of metallic copper and ranged in thickness from 0.002 to 0.020 inch. Foil thicknesses were based on measured foil weights and a copper density of 8.94 gm/cm³. The activated foils were counted on a scintillation counter system using sodium iodide (Tl) crystals.

The 5-minute activity of Cu⁶⁵ was counted at an integral bias of 0.6 Mev in order to minimize background from the 0.51-Mev positron annihilation radiation of Cu⁶³. Bare and cadmium-covered foils were counted alternately to minimize errors from decay time corrections. Background counts to determine the contribution from the 12.8-hour Cu⁶³ activity during the counting of the Cu⁶⁵ were made approximately 50 minutes after the initial counts and were extrapolated to the initial counting period.

For the Cu⁶³ measurements, the 12.8-hour activity was measured several hours after irradiation at a bias of 0.4 Mev. The small differences in foil thickness were taken into account by simple weight corrections of the activities.

The results of the measurement are tabulated in Table III and are shown graphically in Figure 3. In Table III the column labeled Fuel Position indicates whether the foil pairs were on Spinner "A" or Spinner "B" of Figure 1. The thermal flux depression factors are derived from the measured subcadmium activities of the present experiment, i.e., by ratioing the measured activities with the product of the relative thermal neutron exposure times the foil weight. These factors can be measured to a sufficient accuracy for copper, and, moreover, the calculational method given in Appendix A may be in error for copper because of the high ratio of scattering to absorption cross sections. The column RI_{Eff} gives the number obtained from Equation 8 for the total resonance integral above 0.622 ev including the $1/v$ component. The final column, RI_{Eff}^{Res} , is the total resonance integral minus the $1/v$ component. The values are based on thermal cross sections of 2.0 barns for Cu^{65} and 4.5 barns for Cu^{63} to make them consistent with values given by Dahlberg⁽¹⁴⁾, et al.

Figure 3 shows the variation of effective resonance integral with foil thickness and compares the present measurements to those of Dahlberg⁽¹⁴⁾, et al., and of Bennett⁽¹⁵⁾. In Figure 3, Bennett's integrals have been re-evaluated on the basis of the calculated thickness correction for gold given in Table II and on the basis of the same gold resonance integral and Cu^{65} thermal cross section used in the present report. The values initially quoted by Bennett are based on boron cadmium ratios and are even lower than those shown in Figure 3. The discrepancy between Bennett's results and those of the present experiment is possibly due to a deviation from a $1/E$ flux in the spectrum of the PCTR in which Bennett's measurements were made. The resonance self-shielding factors measured by Bennett for the very thin foils were used to extrapolate the present results to zero thickness. The results of the measurements by Dahlberg, et al., are also indicated. The data points at the origin are Dahlberg's calculated extrapolation to zero thickness. Because their experiment was done in a beam flux, only the extrapolation to zero thickness is directly comparable to the results of the present experiment. The values from the present experiment of 3.17 ± 0.18 and 1.39 ± 0.22 barns compare closely with the values of 3.09 ± 0.15 and 1.38 ± 0.23 barns given by Dahlberg, et al. The major part of the indicated uncertainties lies in the thermal cross sections for copper and in the value of the resonance integral for gold, uncertainties common to both experiments. If these are removed, the relative uncertainties are ± 2 to 3% of the quoted resonance integrals and the comparison is seen to be quite good.

TABLE III
Measured Cadmium Ratios and Resonance Integrals for Cu^{63} and Cu^{65}

Isotope	Experiment	Foil Position (a)	Foil Thickness, inch (b)	Cadmium Ratio	Thermal Flux Depression Factor	RI ^{Tot} , barns (c)	RI ^{Res} , barns (c)
Cu^{63}	I	A	0.0052	17.22	0.993	4.14	2.32 ± 0.06
		A	0.0205	20.20	0.972	3.43	1.60 ± 0.04
	II	B	0.0052	18.31	0.993	4.18	2.36 ± 0.06
		B	0.0205	21.49	0.972	3.46	1.63 ± 0.04
Cu^{63}	III	A	0.00186	15.81	0.998	4.55	2.72 ± 0.08
		A	0.00187	15.90	0.998	4.51	2.68 ± 0.08
		A	0.00423	16.45	0.994	4.34	2.51 ± 0.07
		A	0.00870	18.10	0.988	3.90	2.07 ± 0.04
		B	0.00189	16.61	0.998	4.65	2.82 ± 0.08
		B	0.00191	16.48	0.998	4.70	2.87 ± 0.08
		B	0.00444	18.06	0.994	4.25	2.42 ± 0.07
		D	0.00005	19.39	0.900	3.91	2.08 ± 0.04
Cu^{65}	III	A	0.01013	15.94	0.986	1.98	1.18 ± 0.05
		A	0.01981	16.66	0.973	1.87	1.06 ± 0.05
	IV	A	0.00100	15.05	0.990	2.13	1.32 ± 0.05
		A	0.00423	15.61	0.994	2.04	1.23 ± 0.05

(a) See Figure 1

(b) Based on density of 8.94 gm/cm^3

(c) Based on $\sigma_{th} = 4.5 \text{ barns}$ for Cu^{63} and $\sigma_{th} = 2.0 \text{ barns}$ for Cu^{65} (Ref. 14)

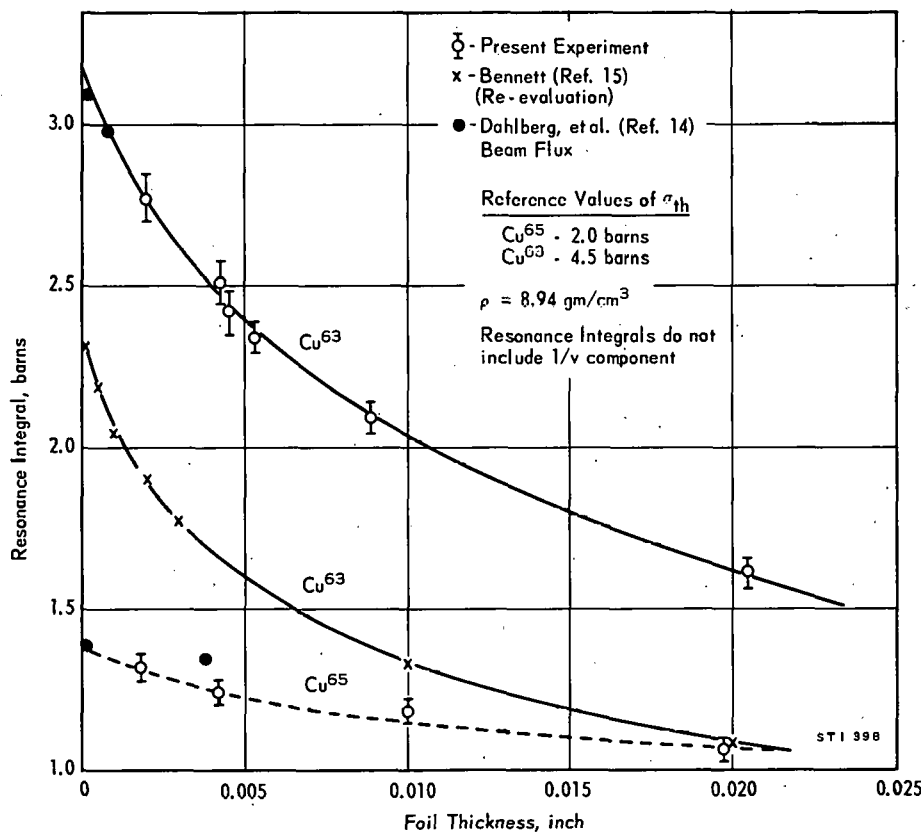


FIG. 3 EFFECTIVE RESONANCE INTEGRAL FOR Cu^{63} AND Cu^{65} AS A FUNCTION OF FOIL THICKNESS (Isotropic Flux in Cavity)

Mo⁹⁸ AND Mo¹⁰⁰

The molybdenum isotopes Mo⁹⁸ and Mo¹⁰⁰ are presumed to be useful as resonance neutron detectors in reactor experiments in that both isotopes have only a single tabulated resonance at an energy of several hundred electron volts and both have a high ratio of resonance to l/v absorption. Under the conditions of the present experiment, these are the only two isotopes of natural molybdenum which give detectable activations.

Foils were made from sheets of molybdenum metal with a nominal thickness of 0.0005 and 0.001 inch. Foils thicker than 0.001 inch were obtained by stacking. The activated foils were counted on the standard scintillation counter system. The counting procedure was somewhat complex because of the two-step decay schemes of the activated isotopes. The Mo⁹⁹ formed from neutron capture by Mo⁹⁸ primarily decays with a 67-hour half-life by β and (β, γ) emission to an isomeric state in Tc⁹⁹. This isomeric state in turn decays with a 6.0-hour half-life to the ground state of Tc⁹⁹ by emission of an 0.14-Mev gamma ray. The Mo¹⁰¹ formed from neutron capture by Mo¹⁰⁰ decays with a 14.6-minute half-life by (β, γ) emission to the ground state of Tc¹⁰¹. This isotope in turn decays with a 15-minute half-life by (β, γ) emission to the ground state of Ru¹⁰¹.

Because of the complicated time behavior of the Mo¹⁰⁰ activations, a reference foil technique was used to measure the time decay characteristics for each experiment. Pairs of cadmium-covered and bare foils were counted alternately to minimize the magnitude of the time correction for each pair. In order to simplify the background correction for the unwanted activity from the Mo⁹⁸, it was necessary to bias above the 0.14-Mev gamma-ray energy of the isomeric state of Tc⁹⁹. A bias of 0.200 Mev was determined to be suitable and a simple exponential time correction with a 67-hour half-life then used for the background correction.

The activity of the Mo⁹⁸ was counted one to two days after the irradiation to minimize possible contamination by activation of Mo⁹² with its 6-hour half-life. A bias of 0.100 Mev was used to increase the count rate by including the gamma rays from the isomeric transition in Tc⁹⁹. During the same interval the foils were counted at a bias of 0.200 Mev to provide the background data for the short-lived activity.

The experimental results are shown in Table IV and Figure 4. Resonance integrals were computed directly by Equation 8 for thermal cross sections of 0.18 ± 0.02 barn for $\text{Mo}^{98(14)}$ and 0.199 ± 0.005 barn for $\text{Mo}^{100(16)}$. The computed thermal flux depression was negligible for the range of foil thicknesses used. The indicated uncertainties in Figure 4 are for the present experiment and do not include errors in thermal cross sections or in the resonance integral of gold. The curves shown on Figure 4 are normalized to the experimental data, but their shape was calculated from listed resonance parameters⁽¹⁾ for the single tabulated resonance of each isotope using the procedure given in Appendix A. Even though, as discussed later, the absolute values of the calculated resonance integrals did not agree with those measured, the calculated depression factors fit the data quite well.

Figure 4 also includes a comparison of the present experiment with other measurements. Dahlberg⁽¹⁴⁾, et al., extrapolate their measurements on Mo^{98} to a zero thickness resonance integral of 10.7 ± 2.5 barns compared to the value of 9.9 ± 1.1 barns obtained from the present experiment. It seems probable, however, that their extrapolation to zero thickness is in error. If the resonance flux depression factor for their beam experiment is calculated from the same

TABLE IV
Measured Cadmium Ratios and
Resonance Integrals for Mo^{98} and Mo^{100}

Isotope	Experiment	Foil Position ^(a)	Foil Thickness, inch ^(b)	Cadmium Ratio	$R_{\text{Eff.}}^{\text{Tot}}$ barns ^(c)	$R_{\text{Eff.}}^{\text{Res}}$ barns ^(c)
Mo^{100}	I	A	0.00052	1.757	3.96	3.87 ± 0.15
		A	0.00091	1.716	4.04	3.95 ± 0.15
		A	0.00189	1.768	4.01	3.92 ± 0.12
		A	0.00382	1.743	3.88	3.79 ± 0.12
		B	0.00052	1.699	4.18	4.09 ± 0.15
		B	0.00091	1.760	4.23	4.14 ± 0.15
		B	0.00189	1.769	4.17	4.08 ± 0.12
		B	0.00286	1.844	3.94	3.87 ± 0.12
Mo^{100}	II	A	0.00052	1.722	4.13	4.04 ± 0.15
		A	0.00091	1.729	4.10	4.01 ± 0.15
		A	0.00286	1.756	3.95	3.86 ± 0.12
		B	0.00091	1.763	4.23	4.14 ± 0.15
		B	0.00189	1.763	4.23	4.14 ± 0.15
Mo^{98}	I	A	0.00052	1.272	9.93	9.85 ± 0.12
		A	0.00091	1.282	9.67	9.59 ± 0.12
		A	0.00189	1.292	9.25	9.17 ± 0.12
		A	0.00382	1.303	8.93	8.85 ± 0.10
		B	0.00052	1.293	9.96	9.88 ± 0.12
		B	0.00091	1.300	9.73	9.65 ± 0.12
		B	0.00189	1.306	9.54	9.46 ± 0.12
		B	0.00286	1.314	9.29	9.21 ± 0.10

(a) See Figure 1

(b) Based on a density for molybdenum density of 10.2 gm/cm^3

(c) Based on $\sigma_{\text{th}} = 0.199 \pm 0.005$ barn for Mo^{100} (Ref. 17) and $\sigma_{\text{th}} = 0.18 \pm 0.02$ barn for Mo^{98} (Ref. 14). Indicated probable errors are for present measurements only and do not include thermal cross section and gold resonance integral uncertainties.

resonance parameters which fit the present experiment, an infinite dilution resonance integral of 9.8 barns is obtained from their data. This agrees very closely with the present results. As in the case of copper, the experimental uncertainties for comparison between experiments are much smaller than the absolute uncertainties.

Thermal cross sections and resonance integrals for Mo⁹⁸ and Mo¹⁰⁰ have also been measured by Cabell^(16, 17). For Mo¹⁰⁰ he obtains⁽¹⁶⁾ a thermal cross section of 0.199 ± 0.005 barn and a resonance integral of 3.73 ± 0.20 barns. For Mo⁹⁸ he obtains⁽¹⁷⁾ a thermal cross section of 0.136 ± 0.003 barn and a resonance integral of 6.69 ± 0.13 barns. The 6.69-barn value is increased to 8.85 ± 0.17 barns for a thermal cross section of 0.18 barn. This higher value is shown in Figure 4 so that the different measurements can be compared on a common basis. Cabell's value for the Mo⁹⁸ thermal cross section would reduce all resonance integrals for Mo⁹⁸ in Table IV and Figure 4 by 24.5%. Cabell's values of the resonance integrals for both isotopes are about 10% lower than those of the present experiment and those given by Dahlberg. The difference is believed to be due to a deviation from a $1/E$ spectrum in the neutron flux used by Cabell.

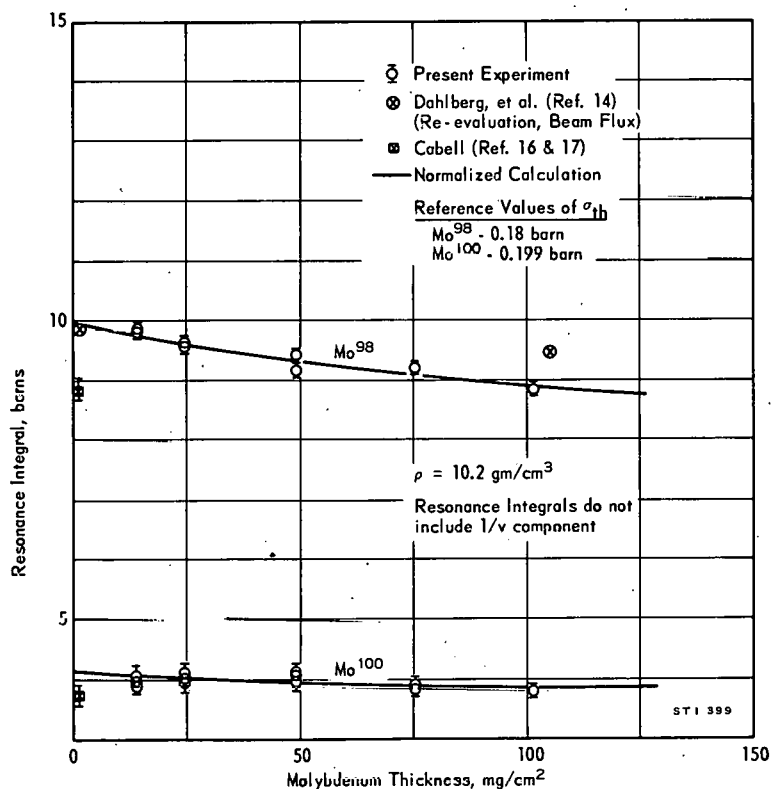


FIG. 4 EFFECTIVE RESONANCE INTEGRAL FOR Mo⁹⁸ AND Mo¹⁰⁰ AS A FUNCTION OF FOIL THICKNESS (Isotropic Flux in Cavity)

It is of interest to compare the calculations of the resonance integral with the measurements. From the tabulation of Hughes and Schwartz⁽¹⁾, Mo⁹⁸ has a single resonance at an energy of 480 ev and Mo¹⁰⁰ has a single resonance at 367 ev. Under these conditions the resonance integral may be calculated from the resonance parameters⁽⁵⁾ or from the thermal cross section⁽¹⁸⁾ by the following relations.

$$RI = 2\pi (E_{th}/E_0)^{\frac{1}{2}} \sigma_{th}/\Gamma \quad (9)$$

$$RI = 4.10 \times 10^6 g \Gamma_n \Gamma_\gamma/\Gamma E_0^2 \quad (10)$$

Here E_{th} is the energy in ev at which the thermal cross section σ_{th} is given, E_0 is the resonance energy in ev, the Γ 's are reaction widths in ev, and g is a weighting factor which is unity for both isotopes of molybdenum. Table V compares measured quantities with calculations made by the above equations and standard values of resonance parameters^(1, 19). The 1/v component is not included.

TABLE V

Resonance Integrals for Mo⁹⁸ and Mo¹⁰⁰

<u>E_0, ev</u>	<u>Resonance Integral, barns</u>		
	<u>Equation 9</u>	<u>Equation 10</u>	<u>Experiment</u>
Mo ⁹⁸ 480	3.9	3.4 \pm 0.9	9.9 \pm 1.1
Mo ¹⁰⁰ 367	3.1	6.2 \pm 1.6	4.06 \pm 0.23

For Mo¹⁰⁰ the measured value lies between the values calculated by the two methods, and appears consistent with the accuracy expected by the two methods. For Mo⁹⁸, however, the measured value is about three times that calculated by either method and is well outside the expected uncertainty of the calculations. This result indicates that a second unidentified resonance is responsible for the major part of the resonance integral of Mo⁹⁸. Because of the size of this resonance it almost certainly is lower in energy than the 480 ev of the identified resonance. This in turn implies that one of the lower energy resonances^(1, 19) for molybdenum is misidentified or that an accidental coincidence of resonances by two isotopes has occurred.

Verification of this assumption is given by an experiment described in Appendix D in which the attenuation of the resonance activation by successive layers of boron absorber is measured. The experimental results suggest that at least half of the resonance integral for Mo⁹⁸ lies in the energy range from 70 to 200 ev. The presence of a lower energy resonance for Mo⁹⁸ has also been observed by Furr⁽²⁰⁾ in a beam transmission measurement. In addition, the experiment described in Appendix D suggests that the effective resonance energy for Mo¹⁰⁰ is considerably higher than the 367 ev of the tabulated resonance. Possible explanations are incorrect isotopic designations of the molybdenum resonances or accidental coincidences of resonance energies. In either event, the present experiment indicates that neither isotope is suitable for use in reactor spectrum measurements in which a single dominant resonance is required.

It is interesting to note from Figure 4 that the resonance flux depression calculated for Mo⁹⁸ from the resonance parameters for the identified 480-ev resonance fits the experimental data very closely. This implies that any second resonance must have approximately the same maximum absorption cross section as the 480-ev resonance. Instead of assuming a second resonance, one may assume that the radiation width, Γ_γ , for the 480-ev resonance is in error, and that instead it should be obtained from the measured resonance integral and Equation 10. The resulting parameters, however, give a calculated flux depression with a slope about four times that shown in Figure 4, which clearly does not agree with the experiment. This gives further evidence of the existence of a second resonance which has a maximum absorption cross section approximately equal to that at 480 ev. Similar arguments can also be advanced for Mo¹⁰⁰.

Na²³

Sodium has two interesting applications for reactor spectrum measurements. First, it approximates the ideal 1/v detector better than any other activating material since the absorption from the single strong resonance is weak compared to the 1/v absorption and since that resonance is at the relatively high energy of 2.85 Kev. Second, the presence of a single resonance at this high energy makes it a useful detector for spectrum measurements in the kilovolt region. Unfortunately, the features that make it useful for one of the two applications are undesirable for the other. In order to make the necessary corrections for either application, it is necessary to know precisely the value of the resonance integral.

For this experiment, foils were made by two different methods. In one method small amounts of sodium bicarbonate were mixed with dental resin, which was then cast into sheets approximately 0.020 inch thick. Half-inch-diameter foils were punched from these sheets. Variations in sodium content were taken into account by reversing cadmium and bare foil positions. A source of error with these foils is the effect of moderation by the contained hydrogen. Neutrons at energies just above the cadmium cutoff energy may enter the cadmium pillbox and be slowed down into the thermal energy region where the capture probability is considerably higher than at the initial epicadmium energy. This effect would cause an increase in activity of the cadmium-covered foils. In order to measure its magnitude, the activities of bare copper foils inside cadmium pillboxes were compared to copper activities obtained when foils of dental resin were included with the copper inside the cadmium pillboxes. With the assumption that the difference in activity was due entirely to slowing into the thermal region, the data for copper were used to calculate the corrections applicable to the sodium foils. These corrections are indicated in Table VI.

A second set of hydrogen-free foils was made by compressing thin cakes of sodium carbonate against aluminum backing foils 0.015 inch thick and 0.5 inch in diameter. Aluminum foil 0.001 inch thick was wrapped around the foils to protect and contain the compressed cakes. When these foils were used, it was necessary to irradiate identical aluminum backing plates and foil covers to make corrections for activities from impurities in the aluminum as well as for the Na^{24} activity resulting from fast neutron capture by aluminum.

The results of the experiment are given in Table VI. Resonance integrals were determined by Equation 8 with a value of 0.52 ± 0.010 barn for the thermal absorption cross section of sodium. No systematic variation in cadmium ratio was noted with foil thicknesses; nor could a thickness correction be simply calculated since the extremely high ratio of scattering to absorption in the sodium resonance invalidates the conditions for which the corrections given in Appendix A apply. For these reasons the value of the resonance integral for sodium is taken to be the average of the values given in Table VI. This average gives a resonance integral of 0.075 ± 0.010 barn compared to the value of 0.07 ± 0.01 reported by Dahlberg⁽¹⁴⁾, et al.

TABLE VI

Measured Cadmium Ratios and Resonance Integrals for Na²³

Experiment	Foil Position	Foil Material	Na Thickness, mg/cm ²	Corrected		RI _{Eff'} barn ^(b)	RI _{Res Eff'} barn
				Mean Cadmium Ratio	Mean Cadmium Ratio ^(a)		
I	A	NaHCO ₃ in dental resin (60 mg/cm ²)	2.7	27.9	29.9	0.270	0.059
	A		2.7	27.7	29.7	0.272	0.061
	A		2.7	27.9	29.9	0.270	0.059
	A		2.7	27.2	29.2	0.277	0.067
	B		2.7	28.4	30.3	0.287	0.076
	B		2.7	28.9	30.8	0.282	0.071
	B		2.7	28.4	30.3	0.287	0.076
II	A	Na ₂ CO ₃ in aluminum envelope	26.0	27.7		0.292	0.081
	A		26.0	27.3		0.297	0.086
	A		26.0	27.7		0.292	0.081
	B		6.5	30.1		0.290	0.079
	B		6.5	29.4		0.297	0.086
	B		6.5	30.1		0.290	0.079
	B		6.5	29.0		0.301	0.090

(a) See text for correction for dental resin.

(b) Based on $\sigma_{th} = 0.520 \pm 0.010$ barn.

The resonance integral for sodium may be calculated from Equations 9 and 10. From the thermal cross section of 0.520 barn (Equation 9), a value of 0.067 barn is obtained. No direct measurements of the parameter Γ_γ could be found in order to calculate the resonance integral from Equation 10. The value given for Γ_γ in BNL-325⁽¹⁾ is also obtained from the thermal cross section by combining Equations 9 and 10. The value given in BNL-325, incidentally, is misprinted. The value of Γ_γ should be 0.54⁽²¹⁾ ev and not 5.4 ev.

U²³⁵ FISSION

The U²³⁵ foils were in the form of an alloy of aluminum and orralloy (93% U²³⁵) with a total foil thickness of 0.010 inch or a U²³⁵ thickness of 5.6 mg/cm². Relative U²³⁵ contents of the foils had been determined by activations in a thermal flux and these uranium concentrations were used to make corrections for the small variations in the foil weights. Activities were obtained on the scintillation counter at a bias of 0.5 Mev. Blank aluminum foils, bare and cadmium covered, were also irradiated in order to make the small correction for activations induced in the aluminum. Comparison experiments made with natural uranium foils demonstrated that, although the U²³⁸ caused a perceptible count in the natural foils, no correction for its activation was required for the orralloy foils.

The measured cadmium ratios for U^{235} fission were 32.0 ± 0.3 for the "A" position and 33.9 ± 0.3 for the "B" position in the SP. Three sets of foils were used for each position with two separate irradiations for each set. Resonance integrals were calculated by Equation 8 with the cross sections and correction factors given below. The calculations showed that for the foil thickness used, the resonance flux depression was negligible, but the thermal flux was depressed by a factor of 0.976. A value of $\sigma_{th} = 577.01$ barns and a g factor of $0.973^{(4)}$ were used, with the g factor based on a neutron temperature of 30°C . The average resonance integral for the two positions is then 267 barns. A calculated correction of 1 barn must be applied to take into account the non-1/v character of the epithermal subcadmium fission cross section in Equation 7. This gives a final value for the U^{235} fission resonance integral of 266 ± 9 barns including all uncertainties other than a deviation of the flux from a 1/E energy dependence. The effective cadmium cutoff energy for U^{235} fissions under these conditions is given by Hardy⁽²²⁾, et al. as 0.60 ev for 0.030-inch-thick cadmium. These authors also report a value of 267 ± 11 barns for the resonance integral of U^{235} fission at a cutoff energy of 0.60 ev. However, a correction for the computed deviation of their spectrum from 1/E reduces their value to 262 ± 11 barns.

Recent measurements⁽²³⁾ in the Thermal Test Reactor (TTR) at Hanford indicate that the effective neutron temperature at the center of the TTR is approximately 40°C above the physical temperature. The g factor at this higher temperature gives a resonance integral 3 barns lower, or 263 ± 9 barns for the present measurement. Of the foil materials in the present experiment, U^{235} is the only one that deviates sufficiently from a 1/v cross section so that the higher temperature would cause a perceptible difference in the measured resonance integral.

The resonance integral for U^{235} fission has also been measured by Clayton⁽²⁴⁾ by two methods, both employing a U^{235} fission chamber. In one case he compared cadmium ratios of the fission chamber with those for a BF_3 counter. From this measurement, he obtains a value of 258 ± 25 barns corrected to a cadmium cutoff energy of 0.60 ev. A second method, based on the fission chamber measurements and slowing down strengths measured by indium foils, gives a value of 271 ± 25 barns at a cutoff energy of 0.60 ev. The results of the present experiment are seen to agree quite well with all of the earlier measurements.

All measurements based on fission product activations of the U^{235} foils implicitly assume that the isotopic distribution of fission products is the same for resonance fission as for thermal fission. Those with a fission chamber do not. Although the assumption is not strictly true⁽²⁵⁾, numerically the error thus introduced is not important. This fact is demonstrated by the observed independence of the measured cadmium ratio of U^{235} fission product activities on the time after irradiation at which the foils are counted.

U^{238} CAPTURE

The resonance integral for U^{238} capture is one of the most important parameters in the design and analysis of thermal reactors using natural or slightly enriched uranium. Many measurements have been made on highly self-shielded uranium rods typical of those used in reactor design. Measurements have also been made on extremely thin foils. Such thin foils are frequently used as the standard whose resonance integral is known (281 barns) in order to make further resonance integral measurements on the highly shielded rods. No prior measurements have been found for uranium foils of intermediate thickness. These intermediate thicknesses are important for providing resonance integral calibrations for foils of the typical thickness used in reactor lattice experiments. In addition, they provide a sensitive check of various methods for calculation of resonance integrals.

Foils were made of uranium depleted to 190 and 350 ppm U^{235} . One set of extremely thin foils was made by depositing uranyl nitrate dissolved in alcohol on foils of filter paper and allowing the solvent to evaporate. The average uranium thickness in these foils was 0.05 mg/cm^2 . Microscopic examination showed that the deposited crystals were extremely small (about 0.01 of the diameter of the individual paper fibers) and that the small crystals were dispersed through the individual fibers rather than on the surfaces. The effect of self-shielding in the individual microcrystals was judged to be negligible. A second set of foils was made from an alloy of 16.0 wt % of the depleted uranium in aluminum. Foils ranging from near 0.001 to 0.020 inch thick were rolled from this material. Additional foil thicknesses were obtained by stacking individual foils. Metallic uranium foils made up the third set of depleted foils. Nominal foil thicknesses of 0.002, 0.006, and 0.010 inch were available.

The activation measurements were obtained by scintillation counting of the 103-Kev X-ray in the 2.3-day decay of Np^{239} leading to Pu^{239} . A single channel analyzer was used with an acceptance width of 90 to 116 Kev. The foils were counted during the time interval from 48 to 96 hours after the irradiation in order to minimize the fission product background. A small correction for the fission product activity was obtained by comparing natural uranium and depleted uranium activities for the uranium metal foils. For the thin foils of uranyl nitrate on filter paper and the foils of uranium in aluminum alloy, cadmium ratios were also obtained with the position of bare and cadmium-covered foils reversed in order to correct for minor variations in U^{238} content of the paired foils.

The results of the measurements are shown in Table VII. For the computation of resonance integrals from the measured cadmium ratios by Equation 8, the quantity $g \sigma_{th}$ for U^{238} was taken to be 2.73 barns. Thermal flux depression factors were negligible for all but the metallic uranium foils. The correction factor for the thickest metal foils was 0.984.

The results are shown graphically in Figure 5. The resonance integrals are plotted against the parameter $\sqrt{S/M}$ where S is the total surface area of the foil, including edges, in cm^2 and M is the total mass in grams of U^{238} in the foil. For U^{238} this parameter has several advantages over the simple thickness parameter used for the preceding isotopes. It gives a scale which conveniently separates the individual measurements for the thin foils and shows the structure in detail. Furthermore, it is the same parameter which is used to coordinate the measurements for thick rods and rod clusters.

In Figure 5, the experimental data are compared to calculations made by the procedure given in Appendix A. The calculations of the resonance flux depression are based on the tabulated resonance parameters⁽⁵⁾ for the nine strongest resonances, which at zero thickness make up 96% of the total resonance integral calculated for all resolved resonances. The calculations include the effect of Doppler broadening of the resonances, but neglect foil edge effects and energy exchanges resulting from resonance scattering. Because of the relatively small ratio of scattering to absorption for U^{238} and because of the thinness of the foils these effects should be small. The calculated curve for slab geometry is seen to fit the experimental data very closely except for the thickest foils where the calculated curve is lower than the measurements. This is just what is expected, though, in that the calculations neglect the

TABLE VII

Measured Cadmium Ratios and Resonance Integrals for U^{238} Capture

Experiment	Foil Position (a)	Foil Material	Cadmium Ratio	Tot RI Eff, barns (b)	Weight of U^{238} , gm	$\sqrt{S/M_1}$ cm/g $^{\frac{1}{2}}$
I	A	Uranyl Nitrate	1.148	277 \pm 3	0.000063	200
	B	On Paper	1.159	278 \pm 3	0.000063	200
II	A	Metal U^{238}	1.939	44.5 \pm 1.5	1.230	1.54
	A		1.893	46.7 \pm 1.5	1.138	1.59
	B		1.770	58.0 \pm 1.8	0.608	2.12
	B		1.735	60.6 \pm 1.8	0.580	2.16
III	A	Metal U^{238}	1.349	117 \pm 2	0.1260	4.52
	A		1.343	119 \pm 2	0.1259	4.52
	A		1.570	72.2 \pm 1.8	0.3561	2.73
	B		1.759	58.8 \pm 2.0	0.6171	2.10
	B		1.731	61.0 \pm 2.0	0.5744	2.18
	B		1.573	77.4 \pm 2.0	0.3535	2.73
IV	A	16 wt % U^{238} in Al	1.185	221 \pm 5	0.0220	11.1
	A		1.172	238 \pm 5	0.0119	14.7
	B		1.201	220 \pm 5	0.0250	10.5
	B		1.215	206 \pm 5	0.0376	9.11
	B		1.196	228 \pm 5	0.0198	11.7
V	A	16 wt % U^{238} in Al	1.150	273 \pm 7	0.00227	33.5
	A		1.152	269 \pm 7	0.00315	27.3
	A		1.153	267 \pm 7	0.00500	22.5
	A		1.150	273 \pm 7	0.00258	31.5
	B		1.162	273 \pm 7	0.00194	35.8
	B		1.181	274 \pm 6	0.01140	15.2
	B		1.159	278 \pm 7	0.00179	37.4
	B		1.157	281 \pm 7	0.00186	36.8
VI(c)	A	16 wt % U^{238} in Al	1.200	205 \pm 5	0.0263	10.3
	A		1.199	206 \pm 5	0.0263	10.3
	A		1.228	180 \pm 6	0.0526	7.62
	A		1.254	160 \pm 6	0.0789	6.39
	B		1.209	211 \pm 5	0.0263	10.30
	B		1.243	182 \pm 6	0.0526	7.62
	B		1.239	185 \pm 6	0.0526	7.62
	B		1.268	164 \pm 6	0.0789	6.39

(a) See Figure 1.

(b) Based on $g \sigma_{th} = 2.73$ barns.

(c) The foils in this set were 0.020-inch-thick nominal and were 0.51 inch in diameter, and consisted of a single foil, or two or three in a stack. See text for a discussion of cadmium covers for the foil stacks.

unresolved resonances and the nonresonant absorption. The relatively small thermal flux depression for these captures becomes important only for the thick foils (low S/M values). At the lower values of S/M, it is of interest to compare the present experimental results with previous measurements on strongly absorbing rods. What are believed to be the most accurate measurements on such rods were those made by Hellstrand⁽²⁶⁾. For values of the total resonance integral including a 1/v component of 1.10 barns Hellstrand gives

$$RI = 4.05 + 25.8 \sqrt{S/M} \quad (11)$$

This expression is shown plotted in Figure 5. Although based on measurements at $\sqrt{S/M}$ values below 1.0, his curve is seen to fit the data of the present experiment over a wide range. In particular the values for the thickest foils are seen to lie precisely on his curve.

The calculated value of the resonance flux depression expected for cylindrical geometry is also shown by the dashed curve of Figure 5. For reactor lattices it is normally assumed that the resonance integral as given by Equation 11 applies equally to rods, tubes, and plates. The curves of Figure 5 show that this is justified for resonance integrals below 50 barns where the two curves coincide. The distinction between the two geometries is, however, seen to be appreciable for higher values of the resonance integral.

The thickest foils of the uranium aluminum alloy foils (Experiment VI of Table VI) required special consideration. The stacks of three 0.020-inch-thick foils, the 0.0789-gm foils of Table VI, were too thick to permit normal closing of the cadmium pillbox. For these foils an additional sheet of 0.010-inch-thick cadmium was wrapped on the edges of the pillboxes. The change of shadow shielding due to the increased size of the cadmium pillboxes is negligible, but changes in the thermal neutron diffusion depressions in the vicinity of the cavity may introduce small systematic errors. An estimate of this effect is included in the experimental uncertainties. In addition, for the thickest uranium-aluminum foils, a correction is necessary for the effect of energy exchange by scattering in aluminum within the foil. In order to estimate the magnitude of this effect, the narrow resonance approximation was used, that is, the effective energy width of the resonance was taken to be small with respect to the maximum energy lost in an elastic scattering of a neutron from an aluminum atom. The calculated correction reduces the resonance integral by 0.5% for the 0.0789-gm foil stack and 0.2% for the 0.0526-gm stack. The effect is therefore negligible for the thinner foils.

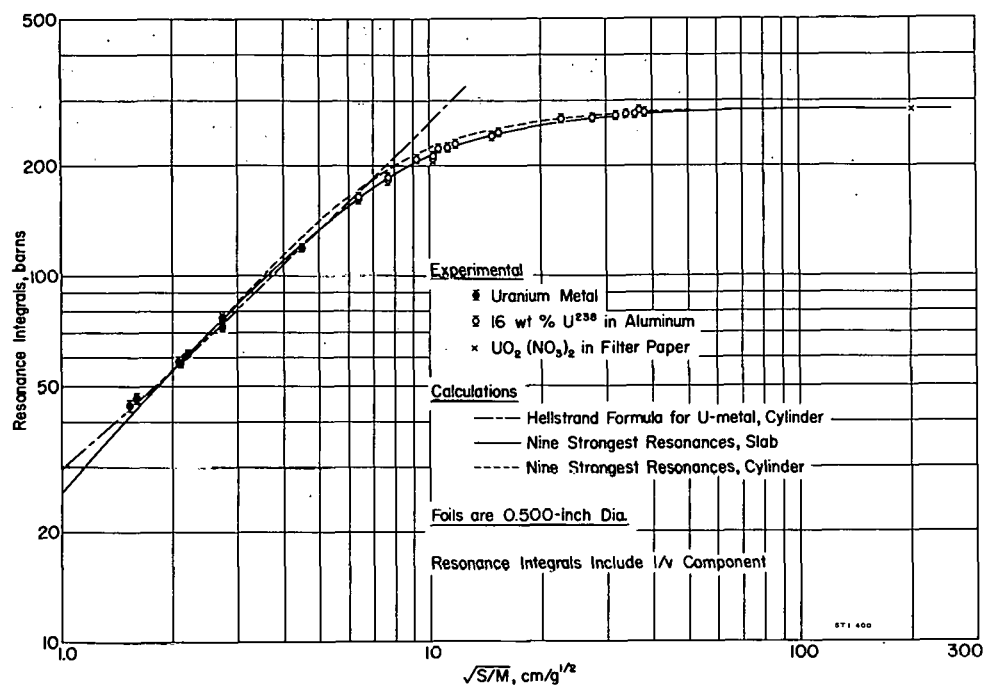


FIG. 5 EFFECTIVE RESONANCE CAPTURE INTEGRAL FOR U^{238} AS A FUNCTION OF FOIL THICKNESS (Isotropic Flux in Cavity)

In¹¹⁵

The experimental determination of the resonance integral of In¹¹⁵ has been re-evaluated from the earlier SRL data⁽⁹⁾ on the basis of the present formalism and cross section values. Only the data for the central irradiation position of the earlier experiment were used. An inspection of the cadmium ratios taken at the two positions used in the earlier experiment indicated a systematic variation with resonance energy as one goes from indium (1.46 ev), to gold (4.9 ev), to tungsten (18.8 ev). This systematic variation is most readily explained by assuming that the epithermal flux deviates from a 1/E dependence for the outermost position, 24 inches from the center of the SP.

Another complication in interpreting the earlier experiments arises because about 80% of the neutron captures in In¹¹⁵ lead to an isomeric state of In¹¹⁶ which decays with a 54-minute half-life by β, γ emission to the ground state of Sn¹¹⁶, and the remaining 20% lead to the ground state of In¹¹⁶ which decays with a 13-second half-life by means of a 3-Mev β particle directly to the ground state of Sn¹¹⁶. Although the branching ratio of the two alternatives is known⁽¹⁾ for thermal neutron capture, it could not be determined from the literature if the ratio was different for epicadmium captures. To determine this relation an

experiment was devised to compare cadmium ratios of the 13-second activity to that of the 54-minute activity for a range of foil thicknesses. The cadmium ratios for the 13-second activities were measured with high precision by the method given in Appendix C. The results of the measurement are shown in Table VIII.

TABLE VIII

Comparison of the Thermal and Resonance Activation Cross Sections for the 13-Second and 54-Minute Activities of In¹¹⁶

Foil Thickness, mg/cm ²	$(\sigma_{13S}/\sigma_{54M})^{\text{Res}}$
	$(\sigma_{13S}/\sigma_{54M})^{\text{Th}}$
2.9	1.020
5.5	1.055
5.6	1.033
4.2	1.009
9.4	1.017
Avg	1.027 ± 0.008

Since no systematic variation with thickness was observed, the average value of the activation ratio was used.

The following relations were used in the re-evaluation of the earlier measurements on the In¹¹⁵ resonance integrals.

$$RI^{54M} = \frac{RI^{\text{Au}}}{(g \sigma_{\text{th}})^{\text{Au}}} F (g \sigma_{\text{th}})^{54M} \frac{[f(\text{CR}) - 1]^{\text{Au}}}{[f(\text{CR}) - 1]^{54M}} \quad (12)$$

$$RI^{13S} = \frac{RI^{\text{Au}}}{(g \sigma_{\text{th}})^{\text{Au}}} F (g \sigma_{\text{th}})^{13S} \frac{(\sigma_{13S}/\sigma_{54M})^{\text{Res}}}{(\sigma_{13S}/\sigma_{54M})^{\text{Th}}} \frac{[f(\text{CR}) - 1]^{\text{Au}}}{[f(\text{CR}) - 1]^{54M}} \quad (13)$$

The following cross sections and measured values were used: RI^{Au}, 1530 barns; (g σ_{th})^{Au}, 99.4 barns; (g σ_{th})^{54M}, 156 barns; (g σ_{th})^{13S}, 38.7 barns; f^{Au}_{In}, 0.985; f^{In}, 0.937 (Ref. 8); (CR)^{Au}, 2.20; (CR)^{54M}, 2.26; and the activation cross section ratios from Table VIII. The factor F takes into account the deviation from 1/v of the indium absorption cross section in the epithermal-subcadmium energy interval. Its value was determined by numerical integration and was determined to be 1.017 for the experimental flux spectrum. The resultant integrals, including the 1/v component, are 2550 ± 80 barns for the 54M activity and 650 ± 30 barns for the 13S activity, or a total activation integral of 3200 ± 100 barns.

The exact calculation of the epicadmium resonance integral is very laborious for a material such as indium where the wing of the resonance extends into the subcadmium region. It can quite readily be approximated, however, by calculating the entire resonance integral by means of Equation 10 for each of the resonances and subtracting from this quantity the excess of the resonance integral over the $1/v$ component in the subcadmium region. This latter value was obtained by numerical integration to give a calculated value of 3190 barns for all resolved resonances and the $1/v$ component for a cadmium cutoff energy of 0.622 ev. This compares with the value of 3213 barns given by Kelber⁽²⁷⁾, and the measured value of 3200 ± 100 barns.

Flux depression factors were calculated for indium by the same procedure as for gold. Only the three lowest resonances contribute perceptibly to the flux depression factor for the foil thicknesses used. The epicadmium $1/v$ component was not considered separately since its resonance integral lies chiefly under the 1.46-ev resonance. The thermal flux depression factors were calculated with a thermal cross section value, σ_{th} , of 191 barns. The results of the computations are given in Table IX and are compared to the earlier SRL measurements⁽⁹⁾ in Figure 6. The agreement is seen to be very good over the entire thickness range. The results of Table IX also agree closely with measurements of the resonance flux depression for indium given by Trubey⁽²⁸⁾.

TABLE IX

Computed Resonance and Thermal Depression Factors
for In^{115} Activations in an Isotropic Flux in a Cavity

Natural Indium Foil Thickness, mg/cm ²	Resonance Depression Factor, F^{Res}	Thermal Depression Factor, F^{th}	F^{Res}/F^{th}
0.05	0.988	1.000	0.988
0.1	0.977	1.000	0.977
0.2	0.959	0.999	0.960
0.5	0.920	0.998	0.922
1.0	0.868	0.997	0.870
2.0	0.796	0.993	0.801
5.0	0.649	0.987	0.658
10	0.519	0.976	0.531
20	0.400	0.956	0.417
30	0.334	0.939	0.357
40	0.294	0.924	0.319
60	0.243	0.897	0.271
100	0.192	0.850	0.226
150	0.156	0.800	0.195
200	0.134	0.759	0.177
250	0.120	0.720	0.167

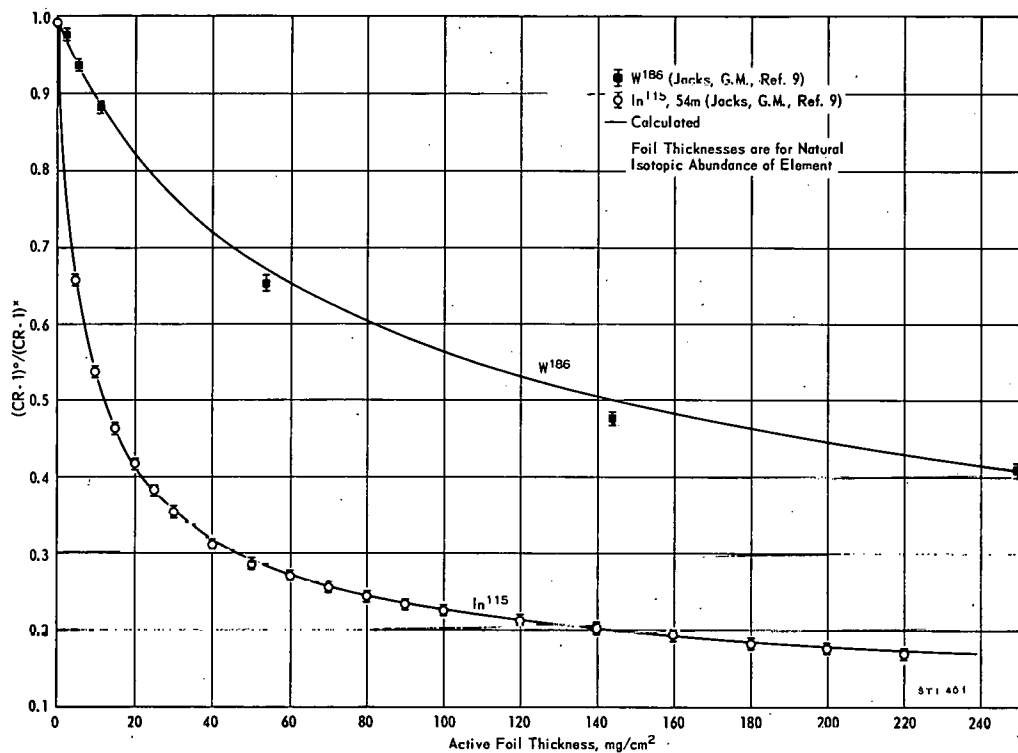


FIG. 6 THICKNESS CORRECTIONS FOR CADMIUM RATIOS OF In^{115} AND W^{186} FOILS
(Isotropic Flux in Cavity)

W^{186}

New activation measurements were made on thin tungsten foils, and the earlier measurements⁽⁹⁾ were re-evaluated on the basis of the present formalism and cross sections. The calculated curve for the flux depression factors is shown in Figure 6 where it is compared to the earlier measurements. The agreement is seen to be good for all but the two intermediate foil thicknesses. Although the discrepancy may be due to an error in the experiments, it is more likely due to the neglect of resonance scattering in the calculation. The ratio of resonance scattering to resonance absorption is much greater than for indium, gold, and U^{238} , for which the agreement was found to be good. The inclusion of scattering would tend to lower the calculated curve. A similar discrepancy, but of even greater magnitude, has been reported by other observers⁽²⁹⁾.

The previously reported resonance integral⁽⁹⁾ of W^{186} has also been re-evaluated. The calculated correction curve of Figure 2 gives an average value of 2.53 for the cadmium ratio of zero thickness W^{186} at the central position as determined from the three thinnest foil pairs. (For the reasons discussed in the section on indium, the 24-inch position was ignored.) Using a thermal cross section for W^{186} of

35 ± 3 barns⁽¹⁾ and making the comparison to the gold cadmium ratio for this location, one obtains a value for the measured resonance integral of 410 ± 40 barns, including the 14-barn 1/v component. Calculations from the resonance parameters⁽¹⁾ for the three strongest resonances by Equation 10 gives a corresponding value of 464 ± 56 barns. Assuming only the 18.8-ev resonance, Equation 9 gives a value of 486 ± 54 barns which becomes 500 ± 54 barns when the 1/v component is included.

Although the discrepancy between calculations and the measured resonance integral are within the combined errors, an investigation was made of possible sources of experimental error. This investigation disclosed that shielding by cadmium could give an erroneously low value for the measured integral. Tabulated resonance parameters⁽¹⁾ show that cadmium has a resonance at 18.5 ± 0.2 ev which partially overlaps and shields the tungsten resonance at 18.8 ± 0.2 ev. Various methods are available for experimentally determining such shielding effects. The method of varying the cadmium thickness⁽⁸⁾ used for gold and indium does not work for overlapping resonances. One method, not used in the present work, is to pair the tungsten foils with foils of a material such as copper for which there is no shielding by cadmium. Normalizations for this method are made by simultaneous activations obtained for the two foil materials in a completely thermalized flux. Another method, the one used here, is to substitute a different filter material for the cadmium, one for which the shielding is negligible or readily calculable. Gadolinium and samarium, which would normally be the best replacements for cadmium, also have resonances near 18.8 ev, so boron was used.

The boron filters used were determined to have an effective B^{10} thickness of 9.1 mg/cm² by means of the experiment described in Appendix D. The tungsten foils consisted of 5 wt % WO_3 dispersed in aluminum at an average tungsten density of 3.0 mg/cm². Cadmium ratios and analogous boron ratios were obtained by the usual irradiation in the SP. The measured geometric mean ratios (from reversing bare and covered foils) were 2.49 for cadmium and 2.83 for boron at "A" position of Figure 1. The measured cadmium ratio used in Equation 8, assuming no resonance shielding, gave a value of 380 ± 40 barns including the 1/v component based on $\sigma_{th} = 35 \pm 3$ barns. The calculated correction to zero thickness gives a corresponding integral of 394 ± 40 barns. The boron cadmium ratio was converted to an idealized unshielded cadmium ratio by the following computed transmission factors: 18.8-ev resonance, 0.76; epicadmium 1/v, 0.1; thermal, 0.030. These depression factors give an equivalent idealized cadmium ratio of 2.20, and by means of Equation 8,

a value for the resonance integral of 473 barns for the actual foil thickness. Correcting to zero thickness gives a value of 490 \pm 50 barns including the 14-barn 1/v component. Comparison of idealized cadmium ratio to the measured one gives a resonance shielding factor of 0.885. Use of this shielding factor in the earlier measurements⁽¹⁹⁾ gives a resonance integral of 506 \pm 50 barns including the 1/v component. This value agrees reasonably well with the present measurement and with the calculated values.

NEUTRON SPECTRUM IN THE SP

The results of the present experiment strongly support the validity of the assumption of a 1/E epithermal flux at the center of the SP. The resonance integrals derived under this assumption show good agreement with measurements taken at other facilities where direct measurements of the spectrum were made^(7,14) or where reliable spectrum calculations could be made⁽²²⁾. The agreement holds from 1.46 ev for indium to 2.85 Kev for sodium and also for U²³⁵ and U²³⁸, which have many resonances distributed over the entire energy range. Such agreement would be most unlikely if there were appreciable deviation from a 1/E spectrum in the SP. Measurements at the center of the TTR⁽¹¹⁾, a facility nearly identical to the SP, also support the assumption.



N. P. Baumann
Experimental Physics Division

APPENDIX A

CALCULATION OF FLUX DEPRESSION FACTORS

THERMAL

Thermal flux depression factors are calculated with Maxwellian-averaged cross sections in the monoenergetic approximation. Here flux depression factors are defined as the ratio of the activity per unit mass of a thick foil to that which an infinitely thin foil of the same material would have had under identical irradiation condition. For an isotropic and monoenergetic neutron flux incident on a slab absorber within a cavity, the average flux depression within the slab is given by the following relation.

$$f_{\text{slab}} = \frac{1 - 2E_3(X)}{2X} \quad (1)$$

Here $X = N \sigma_a$ where N is the atom density of the foil per unit area and σ_a is the microscopic absorption cross section per atom. The E_3 function is the exponential integral over the incident angles discussed in Appendix D. Numerical values for this function are tabulated by Case⁽³⁰⁾, et al. Equation 1 is strictly true only for pure absorption; however, the error introduced by neglecting scattering is appreciable only if the scattering cross section is much larger than the absorption cross section. A plot is given in Figure 7 for use in calculating thermal flux depression factors.

EPITHERMAL 1/v

The monoenergetic depression factor, f_{slab} , of Equation 1 applies at each energy if σ_a varies with energy. For a foil of given thickness the activity of a detector foil, with an activation cross section $\sigma_a(E)$ in an isotropic flux $\phi(E)$, relative to that for an infinitely thin foil in the same flux is given by

$$f = \int f(N, E) \sigma_a(E) \phi(E) dE / \int \sigma_a(E) \phi(E) dE \quad (2)$$

where $f(N, E)$ is given by Equation 1. Equation 2 has been evaluated for a $1/v$ cross section in a $1/E$ flux between the limits of E_c and ∞ . The resultant curve is shown in Figure 7, where the parameter $X = N \sigma(E_c)$. Here N is in the atom density per unit area and $\sigma(E_c)$ is the absorption cross section value at the lower energy limit E_c . The total epicadmium depression is obtained by letting E_c be equal to the effective cadmium cutoff energy. The curve of Figure 7 may also be used to

determine the depression factor for a finite energy interval such as the epithermal subcadmium region. This is accomplished by noting that the depression factors weighted by their respective dilute resonance integrals are additive.

RESONANCE FLUX

Beam Flux, No Doppler Broadening

The problem of the flux depression in an absorbing slab has been solved analytically for a single Breit-Wigner resonance in the absorber with a beam flux at normal incidence to the slab surface^(27,31). A flux constant with energy is assumed. Consider a slab of total thickness X with $N(X)$ atoms per unit area. At a distance X_o from the front face, with $N(X_o)$ atoms per unit area between that point and the front face, the depression at that point is given by

$$f(X_o) = e^{-(X_o/2)} I_o(X_o/2) \quad (3)$$

$$X_o = N(X_o) \sigma_a^{\max} \quad (4)$$

$$\sigma_a^{\max} = \frac{2.6036 \times 10^6}{E_o} \frac{\Gamma_n \Gamma_y}{\Gamma^2} \quad (5)$$

where I_o is a modified Bessel function of the first kind. This function is frequently designated as a Bessel function with an imaginary argument⁽³²⁾ as $J_o(ix)$. The average depression over the whole foil is obtained by averaging Equation 3 over the total foil thickness. The result is

$$f(X) = e^{-(X/2)} \left[I_o(X/2) + I_1(X/2) \right] \quad (6)$$

$$X = N(X) \sigma_a^{\max} \quad (7)$$

where I_1 is also a modified Bessel function of the first kind and is frequently designated⁽³²⁾ as $-i J_1(ix)$. The flux depression factors obtained from Equation 6 are plotted in Figures 7 and 8.

Isotropic Flux, No Doppler Broadening

The flux depression for isotropic flux incidence is complicated by the integration over angles. Such computations have been performed numerically⁽²⁷⁾. Useful approximations are available⁽²⁷⁾ in terms of the effective foil thickness

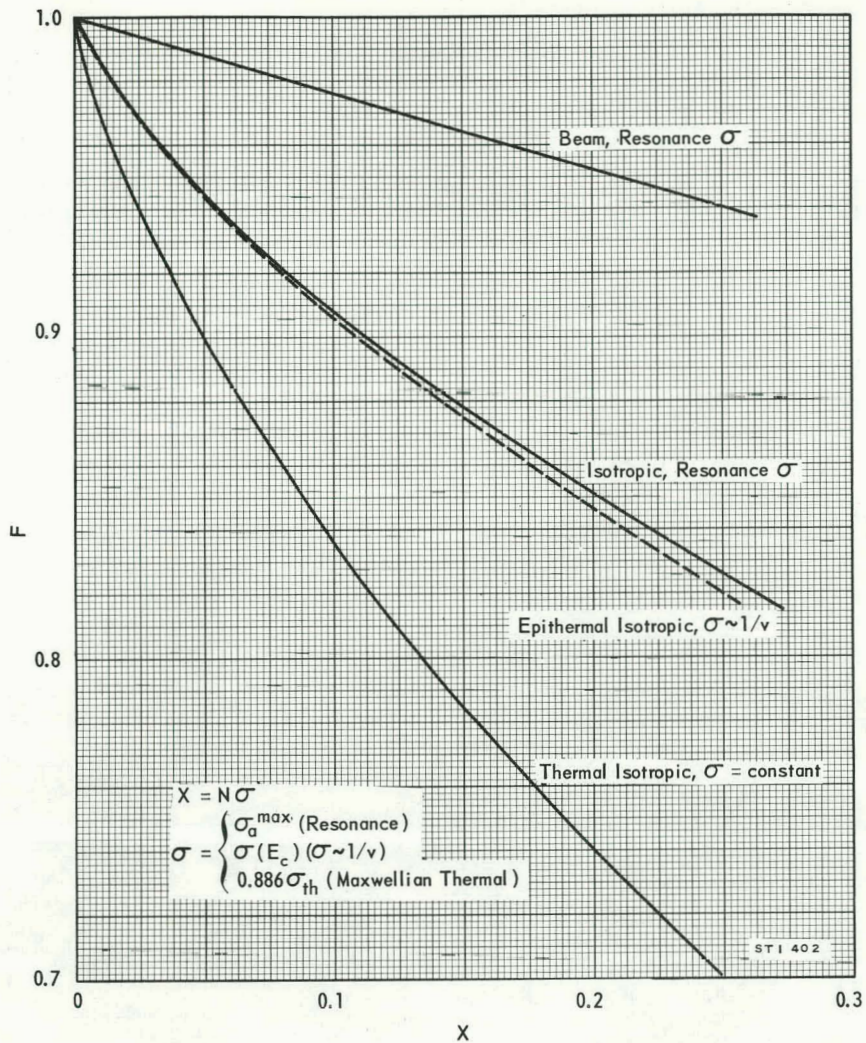


FIG. 7 FLUX DEPRESSION FACTORS FOR THIN FOILS WITH NO DOPPLER BROADENING

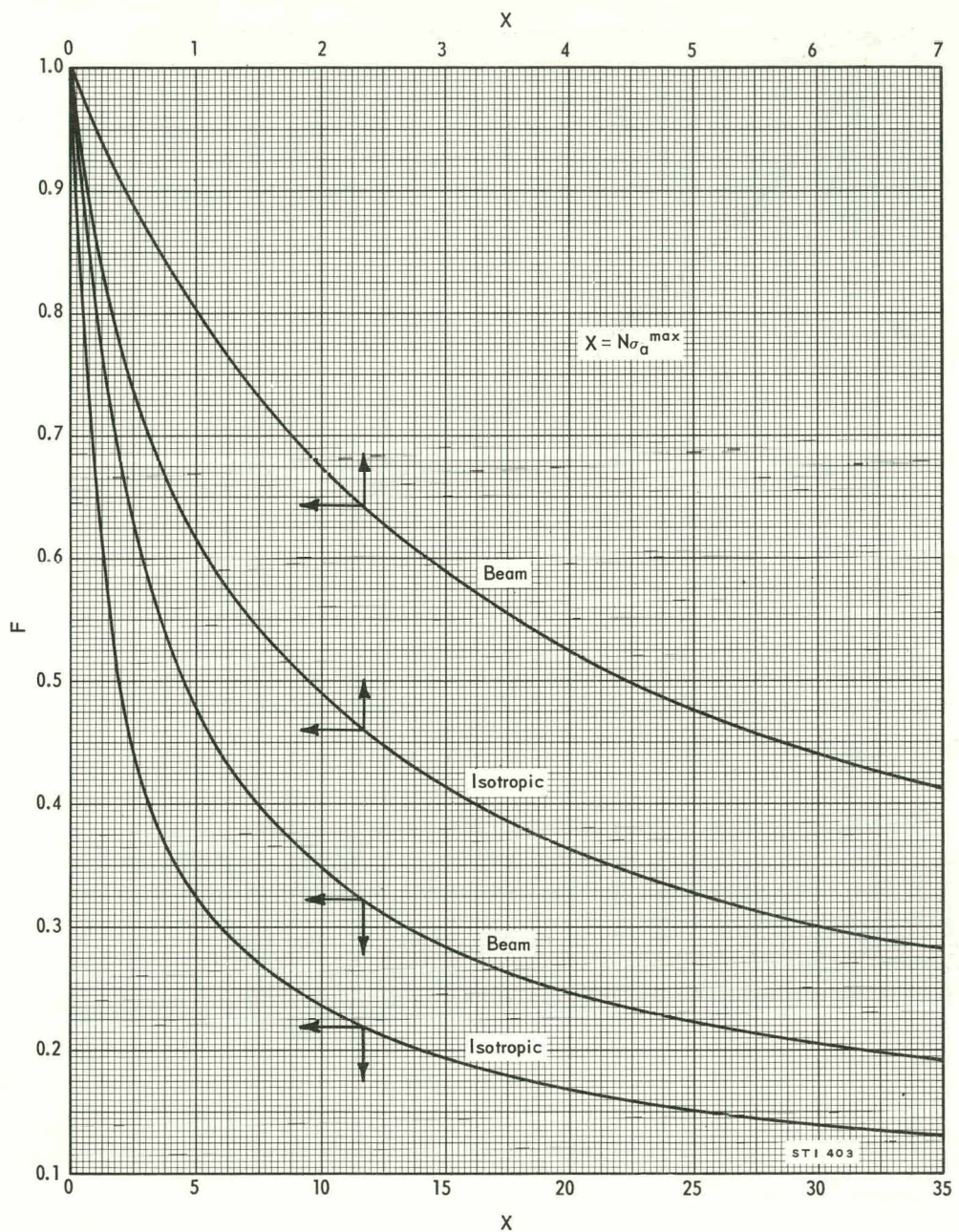


FIG. 8 RESONANCE FLUX DEPRESSION FACTORS FOR THICK FOILS WITH NO DOPPLER BROADENING

$X = N_a \sigma_a^{\max}$, for very thin or very thick foils.

$$f(X) \approx 1 + \frac{X \ln X}{4} - 0.3274X \quad X \ll 1 \quad (8)$$

$$f(X) \approx 1.3333 (\pi X)^{-\frac{1}{2}} \quad X \gg 1 \quad (9)$$

The calculated depression factors are shown in Figures 7 and 8.

Isotropic Flux with Doppler Broadening

Tabulated resonance parameters are given in terms of the relative motion of the neutron and target atom. When it is desired to make calculations in terms of the neutron energy alone, some corrections must be introduced for any motion of the target atoms. Ordinarily this is thermal motion with a Maxwellian velocity distribution isotropic in direction. Here the correction serves to broaden the width and reduce the maximum cross section of the Breit-Wigner resonance. Solutions of the Doppler broadening problem have been obtained in various approximations^(5,6). For the present purpose, the results of computations performed by Roe⁽³³⁾ as presented by Stewart and Zweifel⁽⁶⁾ appear the most suitable. They express these results in terms of the parameter τ , where

$$\tau = \frac{2V}{S} N_a \sigma_a^{\max} \quad (10)$$

Here V is the volume, and S is the total surface area of the absorbing material, N_a is the volume density of absorber atoms, and σ_a^{\max} the peak resonance absorption cross section. For an infinite slab, $\tau = X$ as defined in the preceding section. For foils with a non-negligible edge surface, the more general form is used. With Doppler broadening, the depression factor cannot be calculated from τ alone. The added complexity may be expressed in terms of the single parameter θ ,

$$\theta = \frac{4 E_{th} E_0}{A \Gamma^2} \quad (11)$$

where E_{th} is the temperature of the absorber in units of electron volts, E_0 is the resonance energy, A is the ratio of absorber to neutron masses, and Γ is the total reaction width of the resonance. The results for slab geometries are reproduced in Figures 9 and 10. Note that for $\theta = 0$, these curves coincide with the appropriate curves in Figures 7 and 8. Curves have also been computed for resonance flux depressions in cylinders and spheres with Doppler broadening included^(33,6).

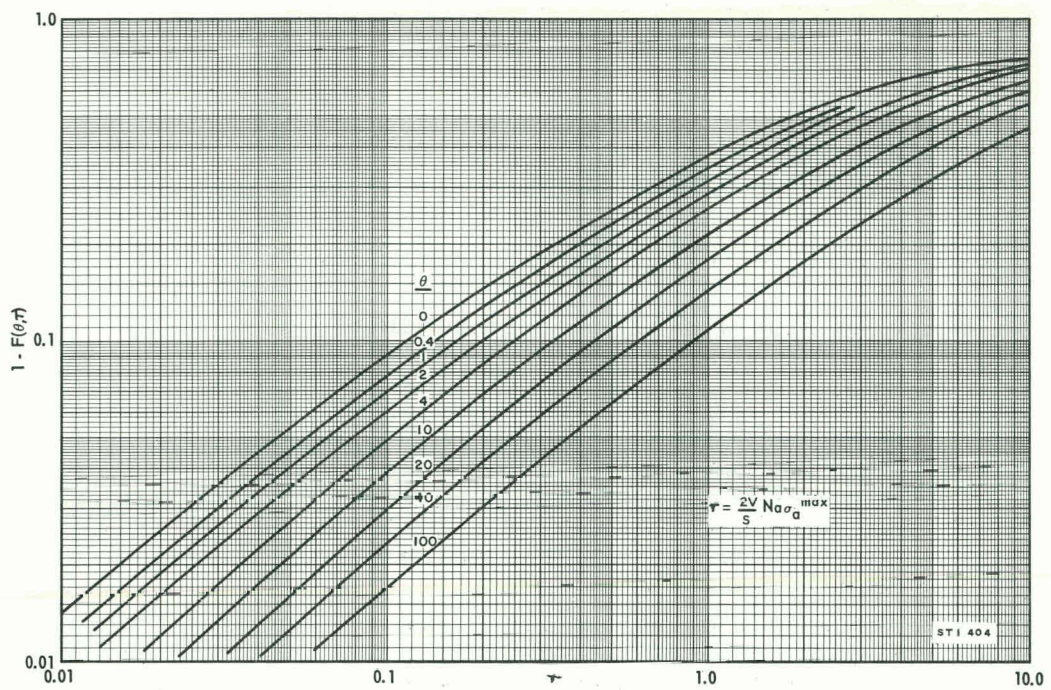


FIG. 9 RESONANCE FLUX DEPRESSION FACTORS FOR THIN FOILS
WITH DOPPLER BROADENING INCLUDED
(From Roe, Ref. 33, and Stewart and Zweifel, Ref. 6)

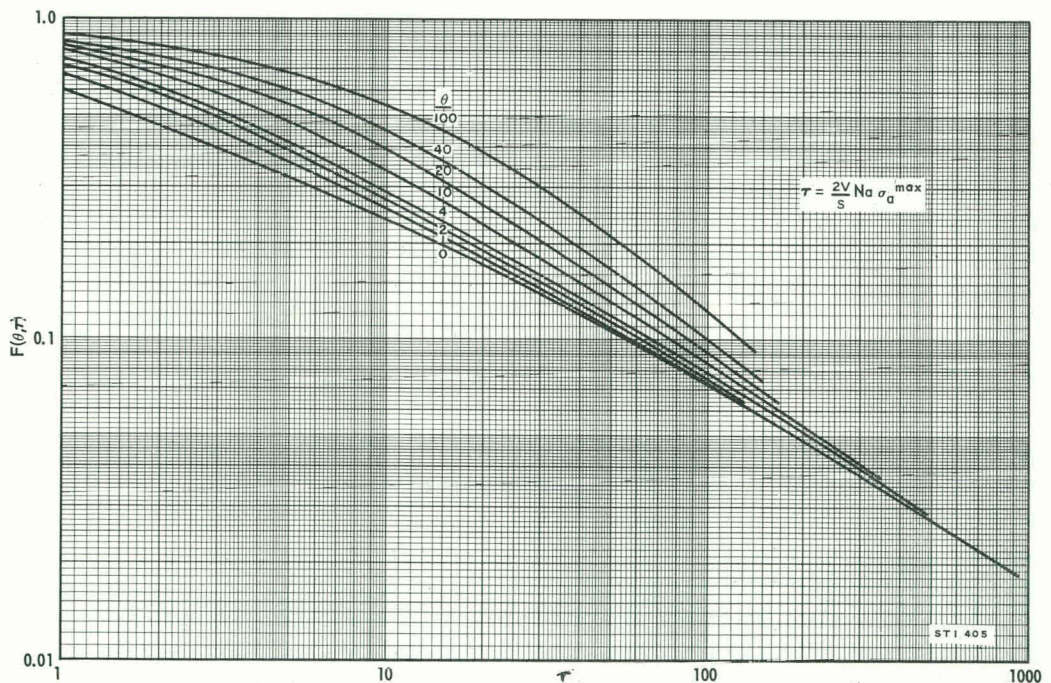


FIG. 10 RESONANCE FLUX DEPRESSION FACTORS FOR THICK FOILS
WITH DOPPLER BROADENING INCLUDED
(From Roe, Ref. 33, and Stewart and Zweifel, Ref. 6)

PAGES 43 to 44

WERE INTENTIONALLY
LEFT BLANK

When the product of the ratios of measured activities is taken, the time factors, f , and the efficiencies cancel out exactly and one has the following expression for the cadmium ratio.

$$\left(\frac{A_1 B_2}{A_2 B_1} \right)^{\frac{1}{2}} = \frac{(\text{Act})_{\text{Bare}}^{\text{Sat}}}{(\text{Act})_{\text{Cd}}^{\text{Sat}}} \equiv \text{Cd Ratio} \quad (5)$$

This method has the advantage that neither the times, nor the time intervals need be known precisely. Simultaneity of time is all that is required.

APPENDIX D

DETERMINATION OF THE EFFECTIVE RESONANCE ENERGY FOR Mo⁹⁸ AND Mo¹⁰⁰

For resonance detectors with one or two strong resonances, the energies of the resonances may be determined by irradiating a set of uniform foils of the detector material in a beam of epicadmium neutrons with varying thicknesses of B¹⁰ absorber material interposed between the foils and the neutron source. For a 1/v absorber such as B¹⁰, the effective absorber thickness, $Y = [N \sigma_a(E)]$, depends on the absorber atom density per unit area, N, and on the absorption cross section, $\sigma_a(E)$, which varies as $E^{-\frac{1}{2}}$. For a single resonance the measured foil activations vary with absorber thickness as $\exp(-Y)$. Since the amount of boron and its thermal cross section are known, measurement of Y uniquely determines the resonance energy. Under ideal conditions of resonance strength and spacing, measurements can also be analyzed to obtain the energies of two or more resonances for a given detector.

Epithermal beam fluxes of sufficient strength to determine the resonance energy of Mo⁹⁸ were not available from the SP so a method was devised for making a similar analysis in an isotropic flux. Consider a detector foil whose effective absorption thickness is $X = N \sigma_a$, where N and σ_a now refer to the detector foil. The foils are encased in a pillbox of B¹⁰ absorber whose thickness on each face is Y, defined as for the beam flux. At a given angle θ to the normal, the incident flux is attenuated by a factor $\exp(-Y/\cos \theta)$ at the detector foil surface and the solid angle of the incident flux is given by $2\pi \sin \theta d\theta$. The effective surface area normal to the direction of incidence is reduced by a factor of $\cos \theta$. The fraction of the neutrons reaching the detector foil which are absorbed in the foil is given by $[1 - \exp(-X/\cos \theta)]$. Combining the terms and cancelling out the constant factor, 2π , one obtains the following relation for the relative activity of an arbitrary thickness foil inside a variable thickness cover.

$$f(X, Y) = \frac{\int_0^{\pi/2} e^{-\frac{Y}{\cos \theta}} \cos \theta \sin \theta (1 - e^{-\frac{X}{\cos \theta}}) d\theta}{\int_0^{\pi/2} \cos \theta \sin \theta (1 - e^{-\frac{X}{\cos \theta}}) d\theta}$$

$$= \frac{2[E_a(Y) - E_a(X+Y)]}{1 - 2E_a(X)} \quad (1)$$

The E functions are the exponential integrals which are tabulated by Case⁽³⁰⁾, et al. They are given analytically as

$$E_n(x) \equiv \int_0^{\pi/2} e^{-\frac{x}{\cos \theta}} \cos^{n-2}\theta \sin \theta d\theta \quad (2)$$

For resonances, Equation 1 depends sensitively on energy since X is proportional to the foil cross section which varies strongly with energy at a resonance. The energy average over a resonance is in general a difficult problem. In the limiting case of an extremely thin foil, Equation 1 becomes $f(X, Y) = E_2(Y)$ and in the limit of a thick (opaque) foil it becomes $f(X, Y) = 2E_3(Y)$. For a detector foil of intermediate thickness, a close approximation to the energy average of X is given by the constant value of X which would give the same resonance self-shielding for a bare foil. This value is obtained from Equation 1 of Appendix A and the measured self-shielding factor.

For the measurement of the effective resonance energy for the molybdenum isotopes, absorbers were in the form of 18 wt % B¹⁰ in aluminum in sheets with a nominal thickness of 0.010 inch. The boron was in the form of finely ground boron powder granules dispersed in the aluminum matrix. The heterogeneous nature of the absorber foils necessitated the determination of the effective absorber thickness for each foil packet. For this purpose, gold foils of thickness 10 mg/cm² and tungsten foils of thickness 52 mg/cm² were placed adjacent to the molybdenum foils inside the absorber pillbox. The natural molybdenum foils had a thickness of 13.5 mg/cm² (0.0005 inch). The pillboxes were made from laminations of 0.625-inch D foils. A cavity for the stack of detector foils was formed by removing an 0.500-inch D disc from the center of one of the larger boron-aluminum foils. Four, three, two, one, or no boron-aluminum foils were then placed on either side of the detector foils. Cadmium discs 0.020 inch thick on both faces completed the cover packet. The irradiations were performed in the air-filled central cavity of the SP. The five foil packs were equally spaced on the rotating aluminum disc described earlier.

The activities of the detector foils were counted on sodium iodide scintillation counters. After correcting for minor variations in foil weights, the activity of each foil relative to the foil covered only by cadmium was determined. These activity ratios are shown in Figure 12. The gold foil activities were used to determine the effective thickness of the boron covers. The curve for the gold foils was calculated from Equation 1 with X = 0.30. Additional curves for gold are

shown in Figure 12 for the limiting cases of very thin and opaque foils to indicate the intermediate thickness of the foils used. The measured gold activities were plotted on the calculated curve to give the effective boron cover thickness. As a check of the method, the measured W^{186} activities were compared to calculations. From Figure 12, the agreement is seen to be well within the experimental errors. The measured molybdenum activities do not agree for either isotope. The most likely explanation of the discrepancy is that each isotope has additional strong resonances other than the single strong resonance tabulated for each^(27,1). For Mo^{100} the experiment indicates further high energy resonances at energies above those of the resolved resonances. For Mo^{98} an additional resonance in the energy range from 70 to 200 ev is indicated. An accidental coincidence of such a resonance with the Mo^{95} resonance at 75 ev or the Mo^{97} resonance at 133 ev seems most likely. The presence of such a low energy resonance for Mo^{98} has also been indicated by experiments performed by Furr⁽²⁰⁾ from the method of boron absorption in beam geometry.

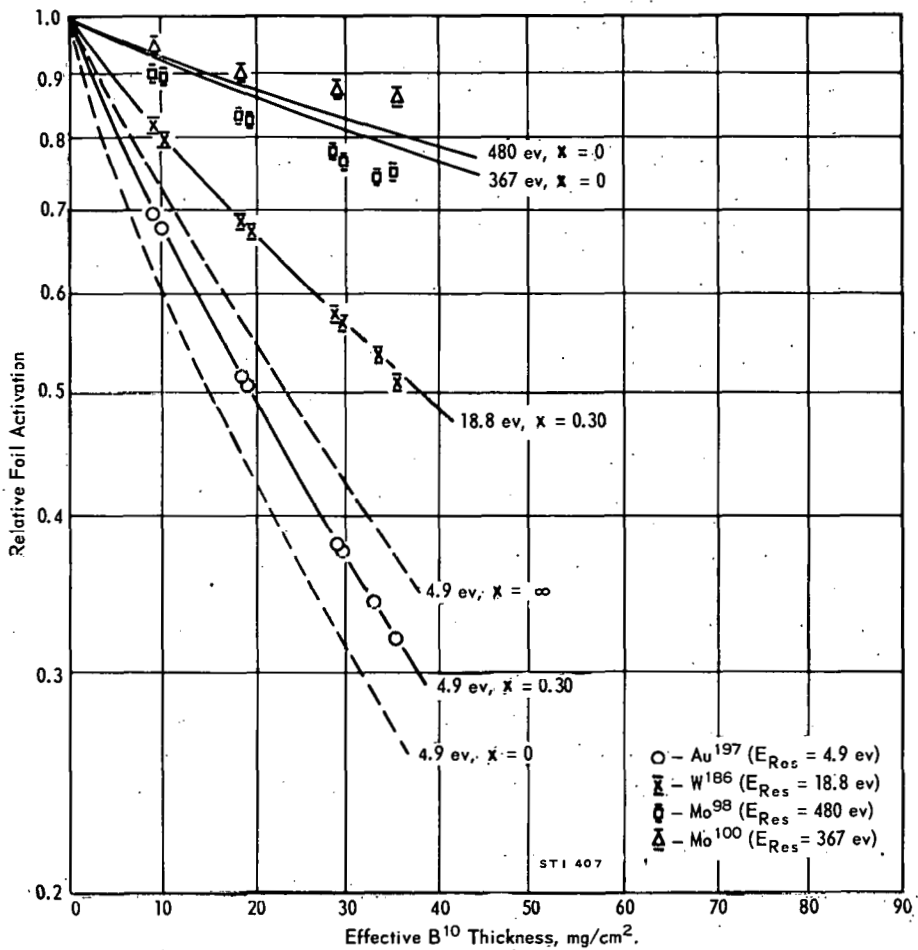


FIG. 12 SHIELDING OF RESONANCE DETECTOR FOILS BY BORON COVERS

BIBLIOGRAPHY

1. Hughes, D. J. and R. B. Schwartz. Neutron Cross Sections. Brookhaven National Lab., Neutron Cross Section Compilation Group, Upton, N. Y. AEC Research and Development Report BNL-325, 2nd Ed., 376 pp. (July 1958); Hughes, D. J., B. A. Magurno, and M. K. Brussel. *ibid.*, BNL-325, 2nd Ed., Suppl. 1, 132 pp. (January 1960).
2. McArthy, A. E., P. J. Persiani, B. I. Spinrad, and L. J. Templin. Neutron Resonance Integral and Age Data. Argonne National Laboratory, Reactor Physics Constants Center, Newsletter No. 1, (June 30, 1961).
3. Macklin, R. L. and H. S. Pomerance. "Resonance Capture Integrals". Proc. U. N. Intern. Conf. Peaceful Uses Atomic Energy, Geneva 5, 97-100 (1955).
4. Westcott, C. H. Effective Cross Section Values for Well-Moderated Thermal Reactor Spectra. Atomic Energy of Canada Ltd., Chalk River, Ont. Research and Development Report CRRP-960, 40 pp. (November 1960). (AECL-1101)
5. Dresner, L. Resonance Absorption in Nuclear Reactors. New York: Pergamon Press, Inc. (1960).
6. Stewart, J. C. and P. F. Zweifel. "A Review of Self-Shielding and Doppler Effects in the Absorption of Neutrons". Proc. U. N. Intern. Conf. Peaceful Uses Atomic Energy, 2nd, Geneva, 16, 652-56 (1958). P/631
7. Jirlow, K. and E. Johansson. "The Resonance Integral of Gold". J. of Nucl. Energy Part A: Reactor Science. 11, 101-07 (1960).
8. Martin, D. H. "Correction Factors for Cd-Covered-Foil Measurements". Nucleonics 13, No. 3, 52-3 (1955).
9. Jacks, G. M. A Study of Thermal and Resonance Neutron Flux Detectors. E. I. du Pont de Nemours & Co., Savannah River Laboratory, Aiken, S. C. AEC Research and Development Report DP-608, 50 pp. (August 1961).
10. Towler, O. A. and J. W. Wade. "Exponential Measurements in Heavy-Water Systems". Chem. Eng. Progr. Symposium Ser. 52, No. 19, 177-81 (1956).
11. Gavin, G. B. "Determination of the Neutron Temperature at the Center of the Thermal Test Reactor". Nuclear Sci. and Eng. 2, 1-13 (1957).

12. Brown, P. S., T. J. Thompson, I. Kaplan, and A. E. Profio. Measurement of the Spatial and Energy Distribution of Thermal Neutrons in Uranium, Heavy Water Lattices. Massachusetts Institute of Technology, Department of Nuclear Engineering, Cambridge, Mass. AEC Research and Development Report NYO-10205, 210 pp. (August 1962). (MITNE-17)
13. Donahue, D. J., R. A. Bennett, and D. D. Lanning. "The Absorption Cross Section of Copper for Thermal Neutrons". Nuclear Sci. and Eng. 7, 184-86 (1960).
14. Dahlberg, R., K. Jirlow, and E. Johansson. "Measurements of Some Resonance Activation Integrals". Reactor Science and Technology 14, 53-4 (1961).
15. Bennett, R. A. "Effective Resonance Integrals of Cu and Au". pp. 26-31 of Nuclear Physics Research Quarterly Report October, November, December 1959. General Electric Co., Hanford Atomics Products Operation, Richland, Wash. AEC Research and Development Report HW-63576, 76 pp. (January 1960).
16. Cabell, M. J. The Thermal Neutron Capture Cross Section and the Resonance Capture Integral of Mo¹⁰⁰. United Kingdom Atomic Energy Authority, Atomic Energy Research Establishment, Harwell, Berks, England. Research and Development Report AERE-R-3239, 12 pp. (January 1960).
17. Cabell, M. J. The Purification and Absolute Determination of Mo⁹⁹ and the Neutron Capture Cross Section of Mo⁹⁸. United Kingdom Atomic Energy Authority, Atomic Energy Research Establishment, Harwell, Berks, England. Research and Development Report AERE-R-3647, 17 pp. (February 1961).
18. Weinberg, A. and E. P. Wigner. The Physical Theory of Neutron Chain Reactions. Chicago: Univ. of Chicago Press (1958).
19. Harvey, J. A., D. J. Hughes, R. S. Carter, and V. E. Pilcher. "Spacings and Neutron Widths of Nuclear Energy Levels". Phys. Rev. 99, 10-36 (1955).
20. Furr, A. K. Private Communication.
21. Lynn, J. E., F. W. K. Firk, and M. C. Moxon. "The 2.85 kev Neutron Resonance of Sodium". Nucl. Phys. 5, 603-14 (1958).

22. Hardy, J., Jr., D. Klein, and G. G. Smith. "The Resonance Fission Integrals of U^{235} , Pu^{239} , and Pu^{241} ". Nuclear Sci. and Eng. 9, 341-45 (1961).
23. Schmid, L. C. and W. P. Stinson. "Neutron Spectrum in the Internal Column of the Thermal Test Reactor". Physics Research Quarterly Report April, May, June 1961. General Electric Co., Hanford Atomics Products Operation, Richland, Wash. AEC Research and Development Report HW-70716, pp. 35-40 (July 1961).
24. Clayton, E. D. Epi-Cadmium Fission in U^{235} . General Electric Co., Hanford Atomics Products Operation, Richland, Wash. AEC Research and Development Report AECD-4167, 29 pp. (December 1955).
25. Glendenin, L. E., K. F. Flynn, and L. M. Bollinger. "Ratio of Symmetric to Asymmetric Neutron Fission of $U-235$ ". Trans. Am. Nucl. Soc. 5, No. 1, p. 20 (1962).
26. Hellstrand, E. and G. Lundgren. "The Resonance Integral for Uranium Metal and Oxide". Nuclear Sci. and Eng. 12, 435-36 (1962).
27. Kelber, C. N. "Resonance Integrals for Gold and Indium Foils". Nucleonics 20, No. 8, p. 162 (1962).
28. Trubey, D. K., T. V. Blosser, and G. M. Estabrook. "Correction Factors for Foil-Activation Measurements of Neutron Fluxes in Water and Graphite". Neutron Physics Division Annual Progress Report for Period Ending September 1, 1959. Oak Ridge National Laboratory, Oak Ridge, Tenn. AEC Research and Development Report ORNL-2842, 204-15 (1959).
29. Bogart, D. and D. Shook. "Self-Shielding in Tungsten Resonances Dominated by the 18.8 ev Strongly Scattering Absorptive Resonance". Trans. Am. Nucl. Soc. 3, No. 2, 461-62 (1960).
30. Case, K. M., G. Placzek, and F. DeHoffman. Introduction to the Theory of Neutron Diffusion. U. S. Government Printing Office, Washington, D. C. (June 1953).
31. Von Dardel, G. and R. Persson. "Determination of Neutron Resonance Parameters from Measurements of the Absorption Integral: Application to the Main Resonance of Uranium-238". Nature 170, 1117-18 (1952).

32. Jahnke, E. and F. Emde. Tables of Functions with Formulae and Curves. New York: Dover Publications (1945).
33. Roe, G. M. The Absorption of Neutrons in Doppler Broadened Resonances. Knolls Atomic Power Laboratory, Schenectady, N. Y. AEC Research and Development Report KAPL-1241, 85 pp. (1954).
34. Westcott, C. H. Effective Cross Section for Well-Moderated Thermal Reactor Spectra. Atomic Energy of Canada Ltd., Chalk River, Ont. Research and Development Report CRRP-787, 29 pp. (1958). (AECL-670)